



SEA LEVEL RISE AND WHAT TO DO by L.C. van Rijn

Content

- 1. What is the Sea Level Rise and what can we expect?**
- 2. Sea surface temperatures (SST)**
 - 2.1 General**
 - 2.2 Sea surface temperatures (SST) during the last interglacial period (LIG)**
- 3. Ice masses**
- 4. Ice melting and sea level rise**
 - 4.1 General**
 - 4.2 Thermal expansion of water**
 - 4.3 Glaciers**
 - 4.4 Greenland**
 - 4.5 Antarctica**
 - 4.6 Total sea level rise**
- 5. What can we do about Sea Level Rise?**



1. What is the Sea Level Rise and what can we expect?

The main causes of Sea Level Rise (relative to the land surface) are:

- melting of ice (polar ice caps, land ice, permafrost, glaciers, etc);
- increased fresh water input by rivers;
- decrease of the fluid density and expansion of volume due to increase of temperature;
- sinking of the land surface.

Sea levels varied over some 150 m during the last 4 glacial periods, see **Figures 1.1** and **1.2**.

Sea level was about 10 m higher than present at about 130 000 years ago.

During the last interglacial period (LIG between 129,000 and 116,000 years ago), the global sea levels were 5 to 10 meters higher than at present.

Some 15,000 to 20,000 years ago during the last glacial period the sea level was about 120 to 140 m lower than at present, see **Figures 1.1** and **1.2**.

Initially, the sea level rise was about 8 mm per year until approx. 7,000 years ago when it slowed down to about 2 mm/year around 2000 followed by an increase to about 3 mm/year at present (2023).

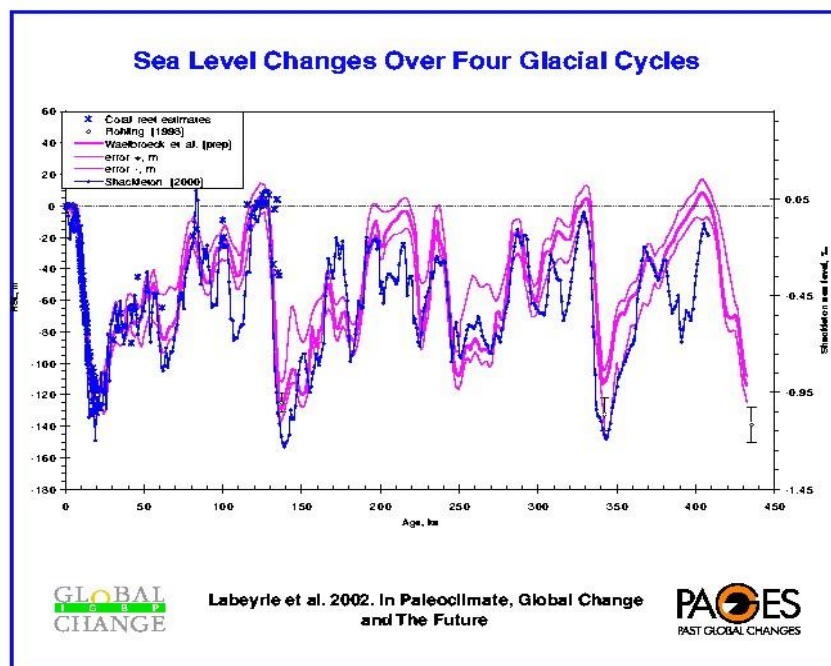


Figure 1.1 Sea level variations on geological time scale (450,000 years); www.geo.uu.nl/fg

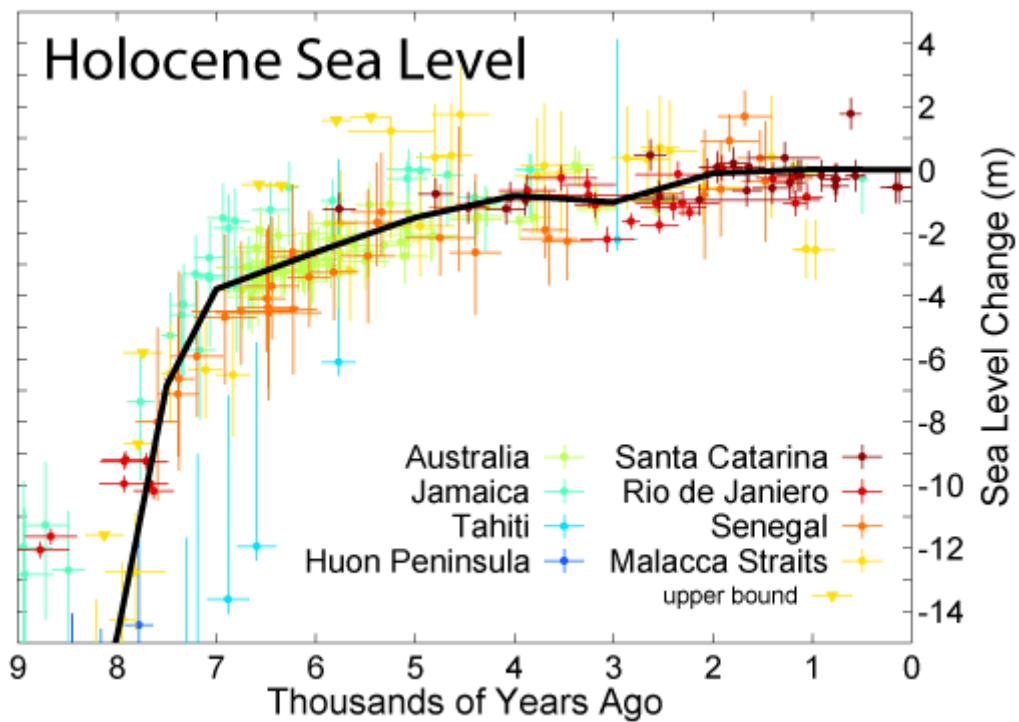
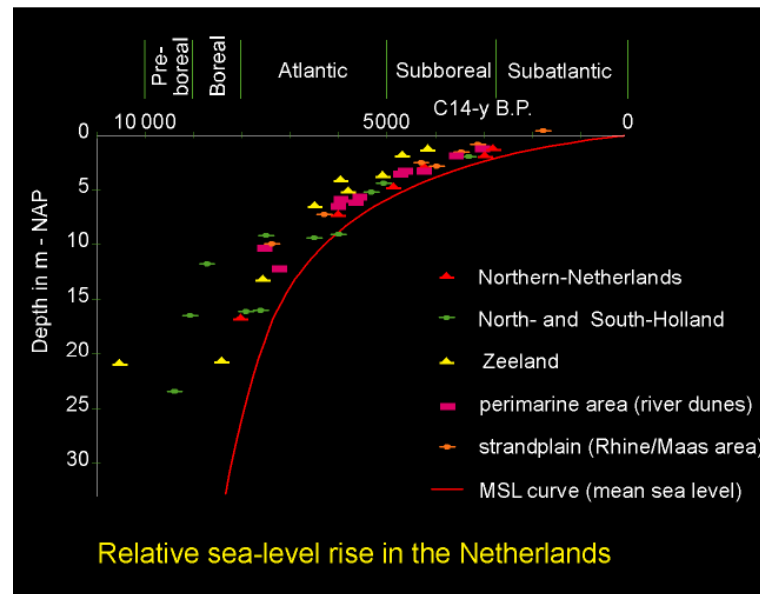


Figure 1.2 *Sea level rise during last 10,000 years*
upper: The Netherlands (www.geo.uu.nl/fg)
Lower: Worldwide (iceagenow.info)



Recent long term data (last 200 years) of Mean Sea Level based on tidal gauges are available for several stations in Europe (Amsterdam, Liverpool, Stockholm); see **Figure 1.3** (IPCC 2001 report). Analysis of these records shows a Sea Level Rise of about 0.2 m for the period between 1900 and 2000. Sea level rise before 1900 was much smaller < 0.1 m. Effects of accelerated Sea Level Rise during the last decade (1990-2000) of the previous century cannot be detected.

At present (2023) the sea level rise for the countries along the North Sea is about 3 mm per year.

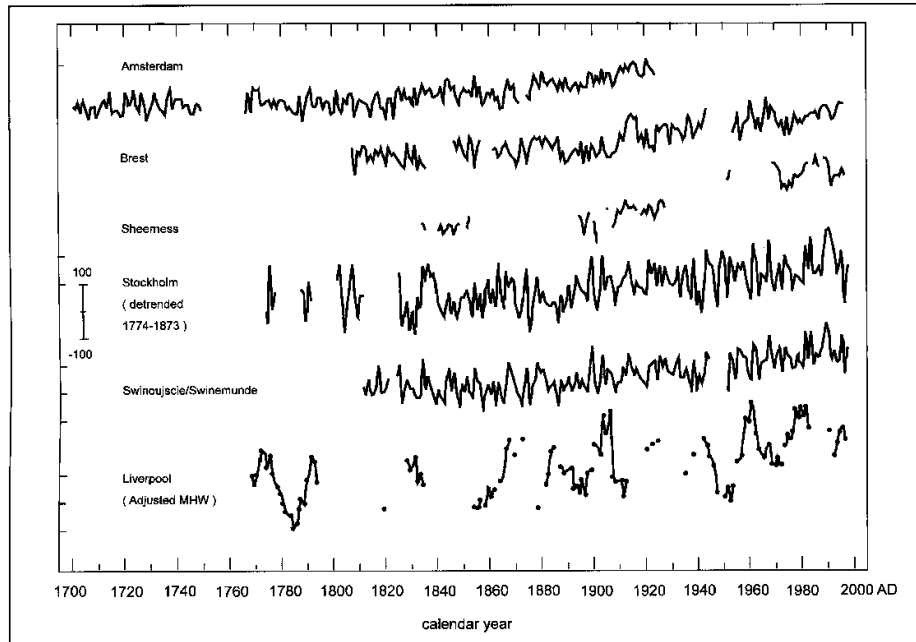


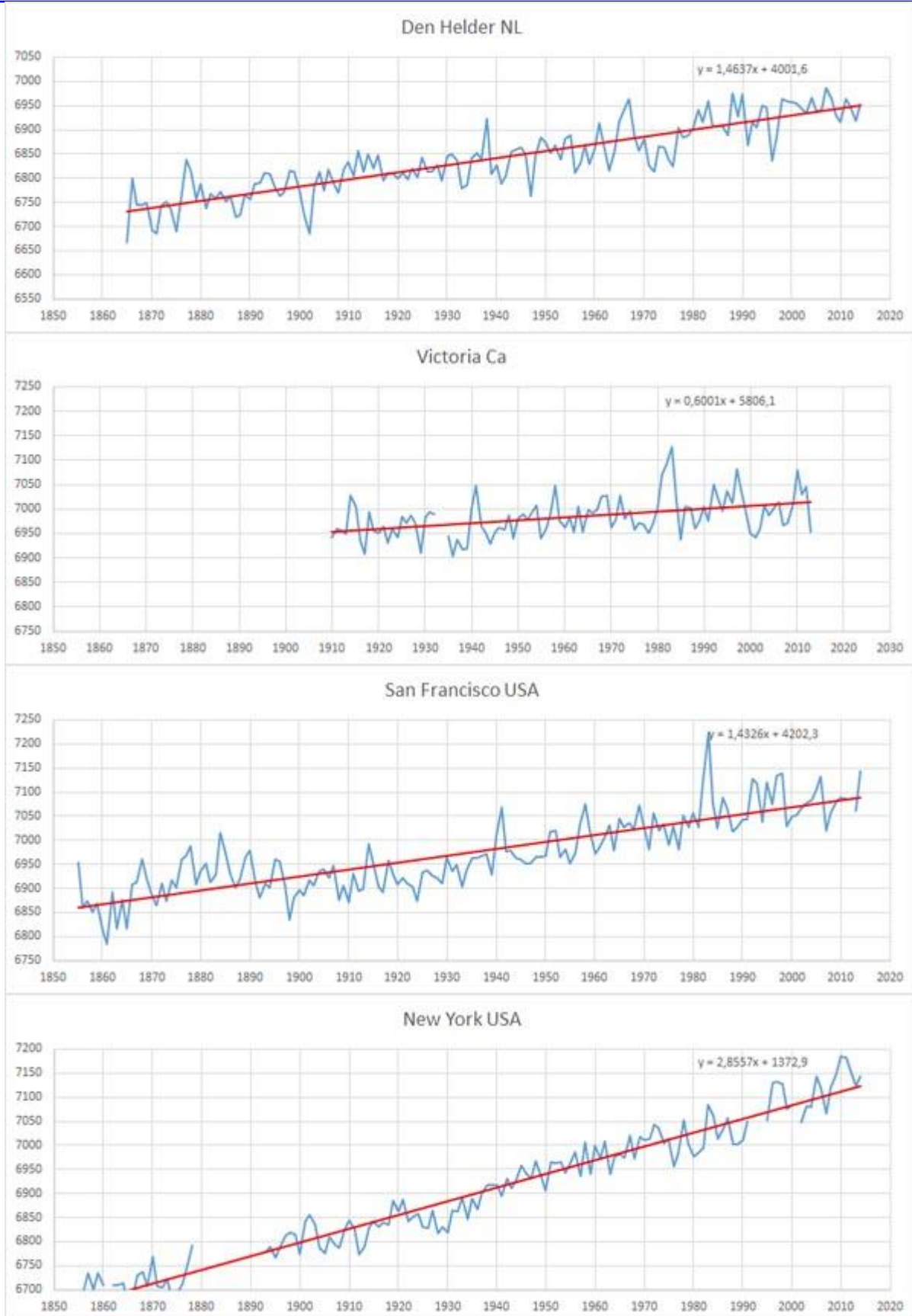
Figure 1. Time series of relative sea level for the past 300 years from Northern Europe. The scale bar indicates ± 100 millimeters. Source: IPCC, 2001.

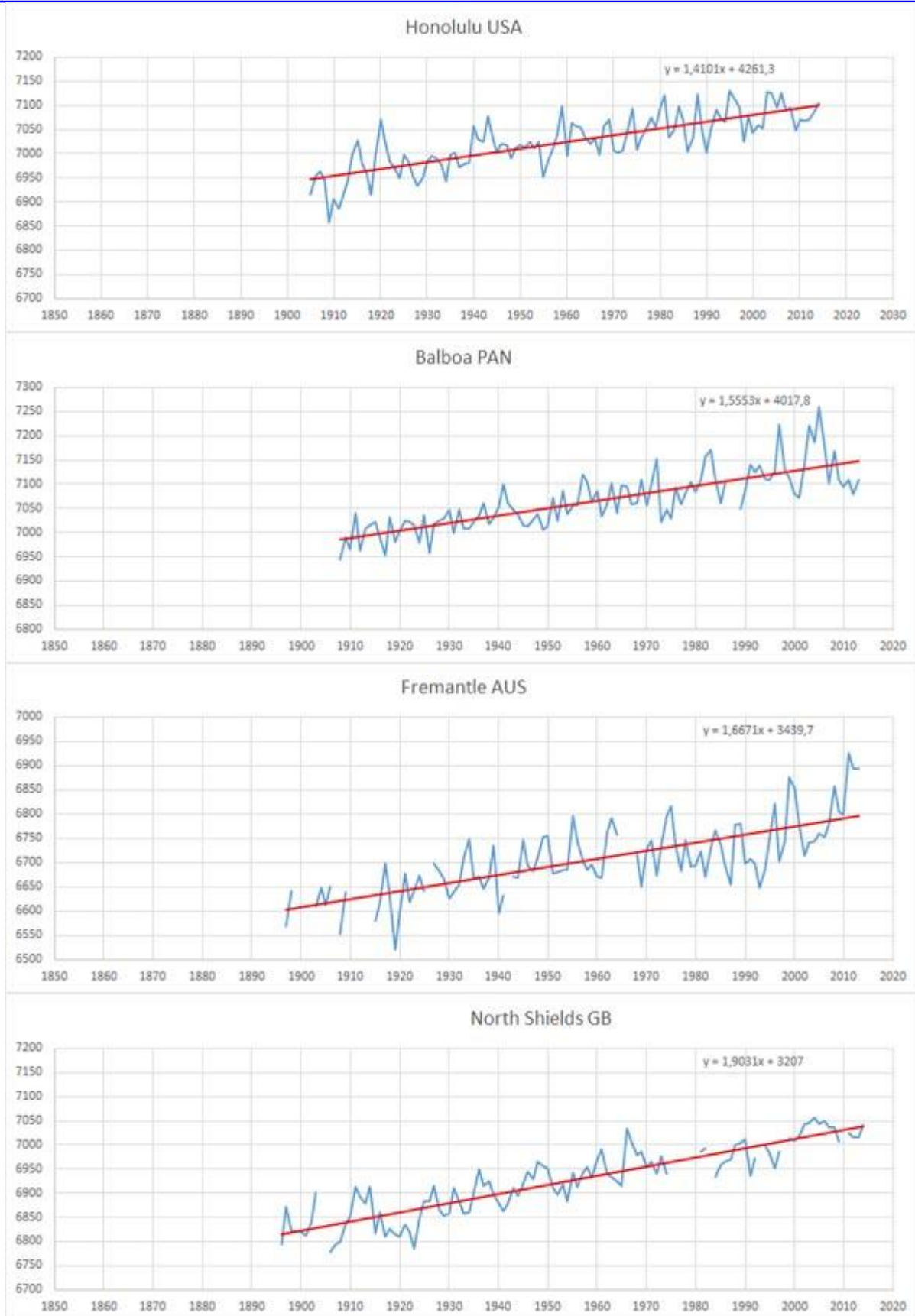
Figure 1.3 Sea Level Rise in Europe between 1700 and 2000 (IPCC, 2001)

Recent analysis of sea level records of 8 global stations (Den Helder, NL; Victoria, Canada; San Francisco, USA; New York, USA; Honolulu, USA; Balboa, Panama; Fremantle, Australië; North Shields, GB; database of www.psmsl.org) shows a fairly constant annual sea level rise in the period 1915 to 2015 (www.klimaatgek.nl), see **Figure 1.4**.

The mean sea level rise of these 8 stations is 1.6 mm per year over the last 100 years (before 2015). Acceleration effects during the last 30 years (1985-2015) cannot be detected.

Figure 1.5 shows the mean sea level of 6 main tidal station in The Netherlands (klimaatgek.nl). The linear trend line gives a value of about 1.8 mm per year between 1890 and 2021. The loess filter over 10 years shows that there are periods with higher and lower values, which are most likely related to variations in wind-related surge levels along the coast.





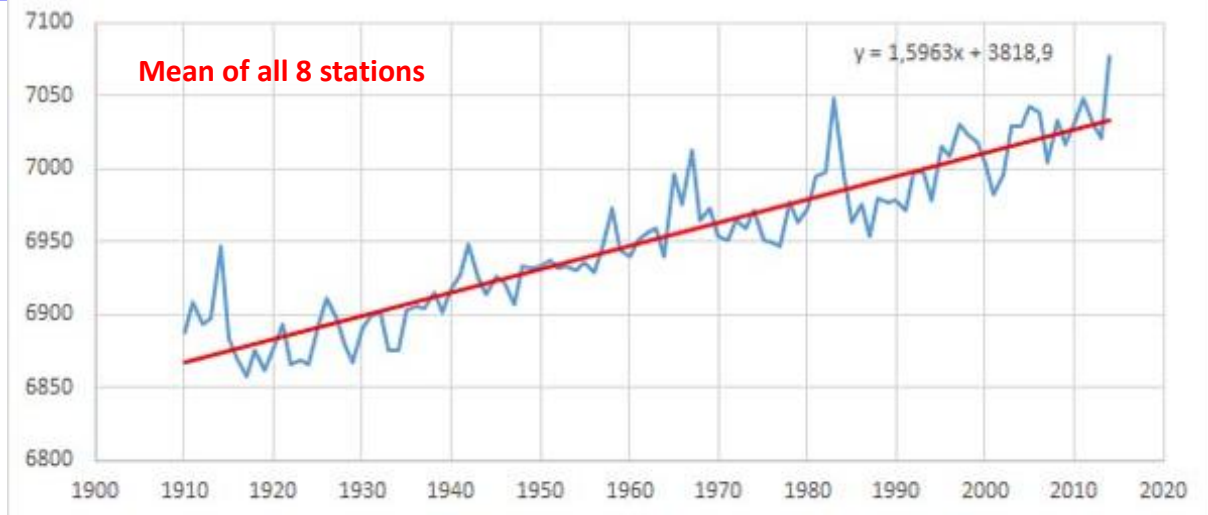


Figure 1.4 Analysis of sea level records at 8 global stations ; period 1910-2015 (www.klmaatgek.nl)
vertical scale: mm's; horizontal scale : years

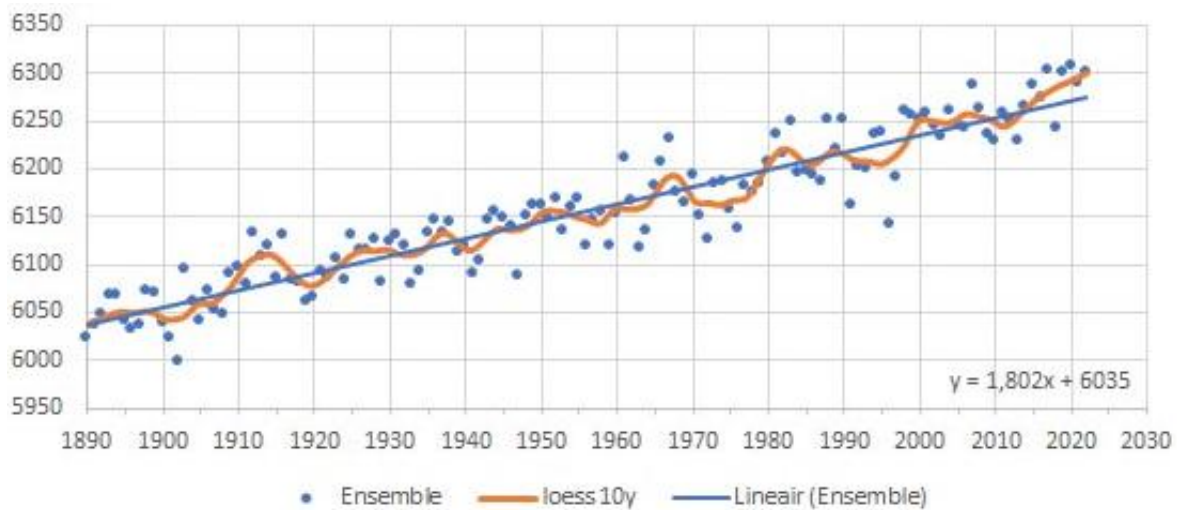


Figure 1.5 Mean sea level of 6 main tidal stations in The Netherlands (*Klimaatgek.nl*)
(*Delfzijl, Harlingen, Den Helder, IJmuiden, Hoek van Holland, Vlissingen*)

Since 1993, the reference global mean sea level (GMSL) based on data from the TOPEX/Poseidon, Jason-1, Jason-2 and Jason-3 missions is estimated, after removing the annual and semi-annual signals and applying a 6-month filter, see **Figure 1.6**.

By applying the postglacial rebound correction (-0.3 mm/yr), the rise in mean sea level has thus been estimated as **3.3 mm/year** (straight line on **Figure 1.6**).

Analyzing the uncertainty of each altimetry correction used in the estimation of the GMSL, as well as a comparison with tide gauges, yields an uncertainty in the GMSL trend of approximately 0.4 mm/year at the 90% confidence level. The uncertainty range (90% confidence level) of the GMSL data at each time step has also been estimated. It is superimposed to the GMSL curve in the figure (shaded area)



Detecting acceleration is challenging, even in such a long record. Episodes like volcanic eruptions can create variability: the eruption of Mount Pinatubo in 1991 decreased global mean sea level just before the Topex/Poseidon satellite launch, for example. In addition, global sea level can fluctuate due to climate patterns such as El Niños and La Niñas which influence ocean temperature and global precipitation patterns.

Deltares (2022) has analyzed the sea level data of at six main tidal stations of the Netherlands (Delfzijl, Harlingen, Den Helder, IJmuiden, Hoek van Holland and Vlissingen). This calculation takes into account the various factors affecting the fluctuations in water levels, the most important being winds and tides, see **Figure 1.7**. The main results are:

- 1.8 ± 0.1 mm/year before 1990;
- 2.9 ± 0.4 mm/year for 1990-2022.

The wind or surge effect is related to long term variations (10 to 30 years) of the wind climate which leads to long term variations of the wind-related surge levels along the Dutch coast. These oscillations of 10 to 30 years cancel out on a time scale of 100 years, but are important on the short term. Including this effect, the sea level rise at present is about 3 mm/year since 1993 as we are now in a cycle with relatively low wind-related surge (red area of **Figure 1.8**). It is noted that the long term mean sea level rise of 1.8 mm before 1990 also consists of periods with lower and higher sea level rise values. Again, on the very long term these oscillations will cancel out provided no systematic change of the wind climate.

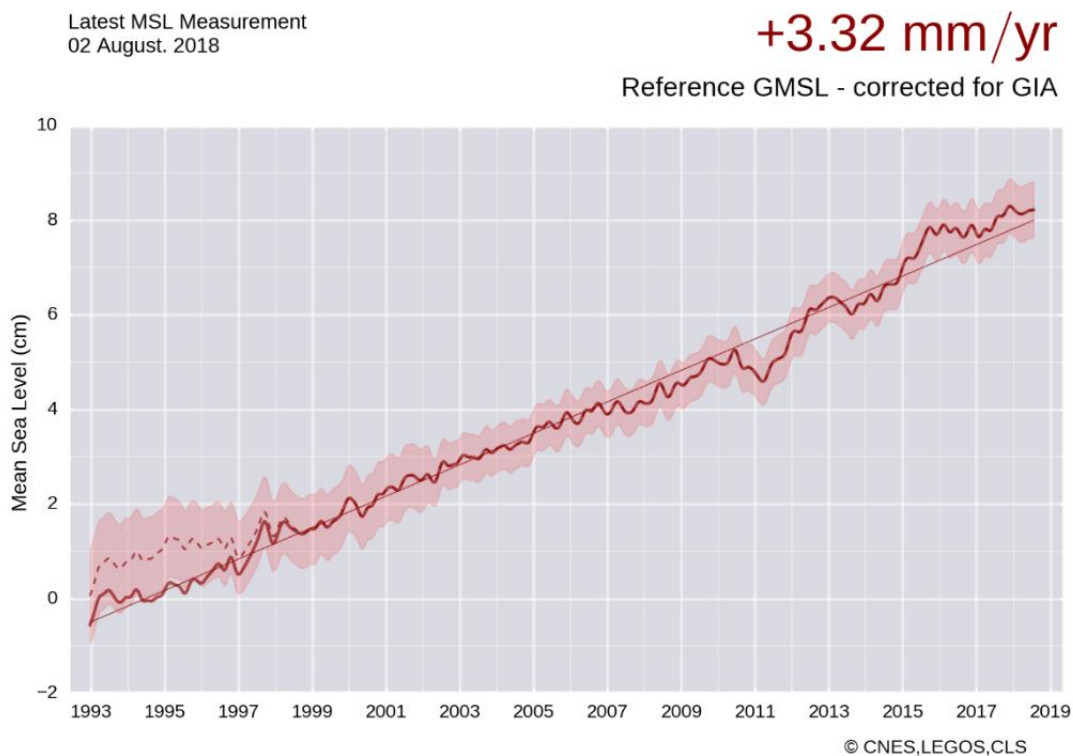


Figure 1.6 Mean sea level based on satellite data (www.aviso.altimetry.fr)

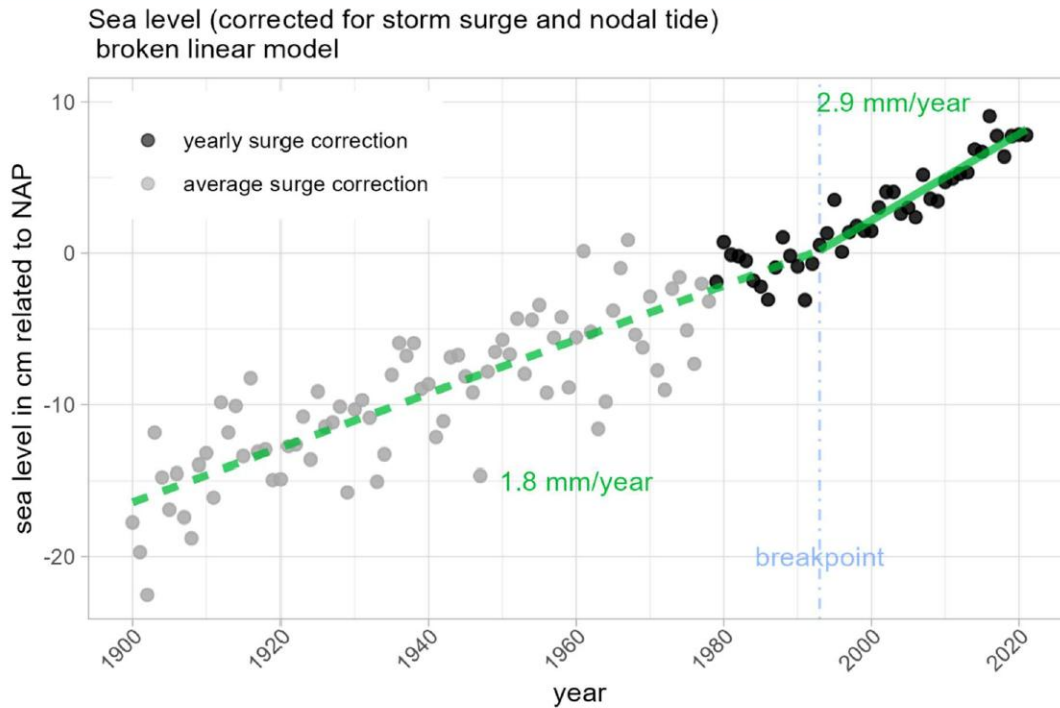


Figure 1.7 Sea level change in The Netherlands over period 1900 to 2020 (Deltares, 2022)

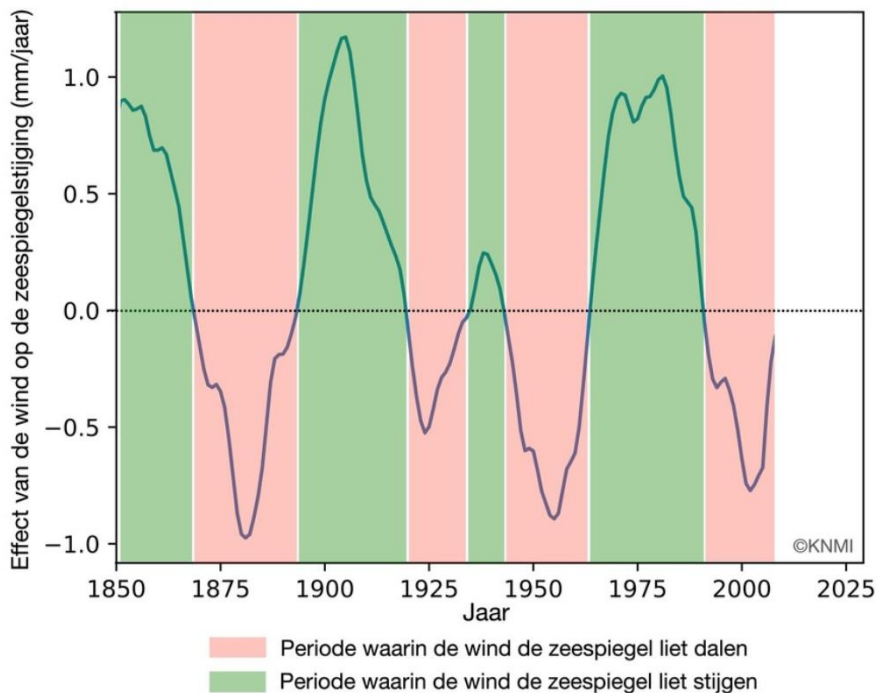


Figure 1.8 Variational component of wind-related surge level at Dutch coast (KNMI.nl/klimaatdashboard, 2024)

In The Netherlands, the sinking of the land surface is of crucial importance for relative sea level rise. It is noted that relative sea level rise remains zero if the land surface rises at the same rate as the sea level and doubles if the land surface sinks at the same rate as the rise of the sea level.

Figure 1.9 shows the sinking rates in the period of 2000 to 2050 (based on TNO, 2018). The sinking along the coastal defense zone with natural sand dunes and sea dikes is relatively small with values of about 2.5 to 5 cm per 50 year (0.05 to 0.1 m/century). The sinking is most pronounced in the peaty polders with values up



to 0.5 m/century, which increases the required pumping capacity (larger difference between outside and inside water levels).

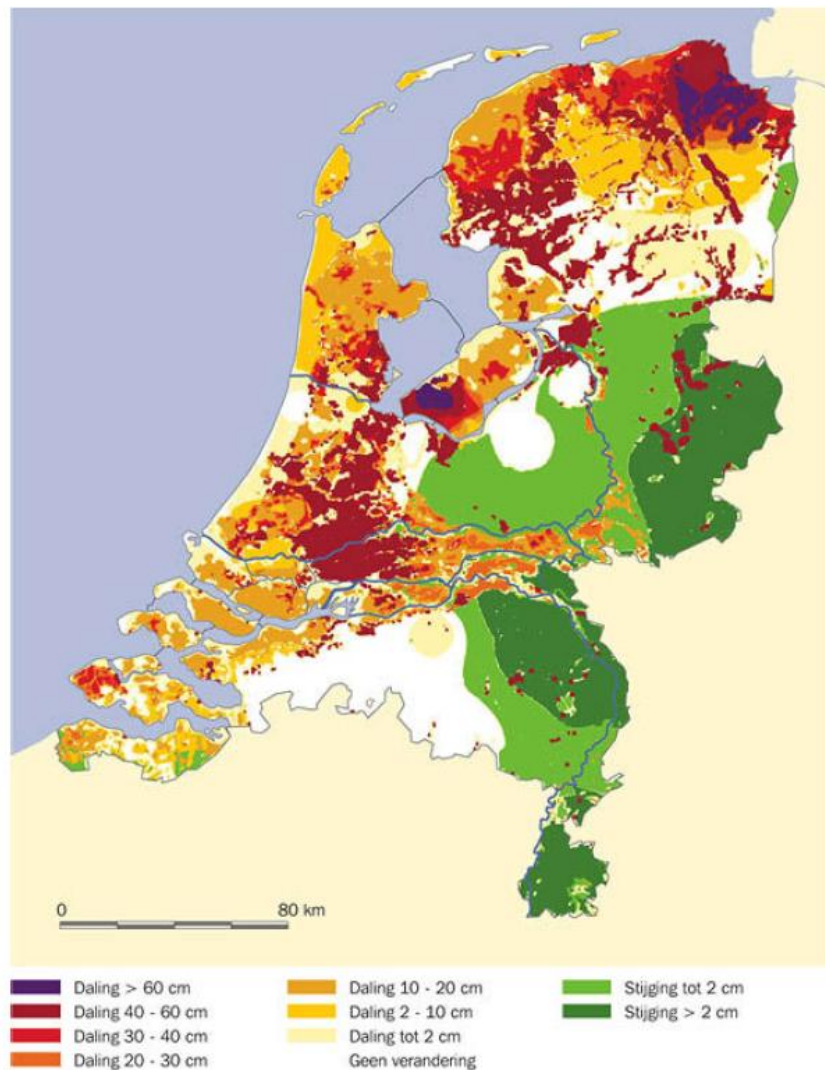


Figure 1.9 Land sinking in period 2000 to 2050, The Netherlands (TNO, The Netherlands)



2. Sea surface temperatures (SST)

2.1 General

Earth's climate is warming. Temperature data showing rapid warming in the past few decades, see **Figure 2.1**. According to NASA data, 2016 was the warmest year since 1880, continuing a long-term trend of rising global temperatures. The 10 warmest years in the 138-year record all have occurred since 2000, with the four warmest years being the four most recent years.

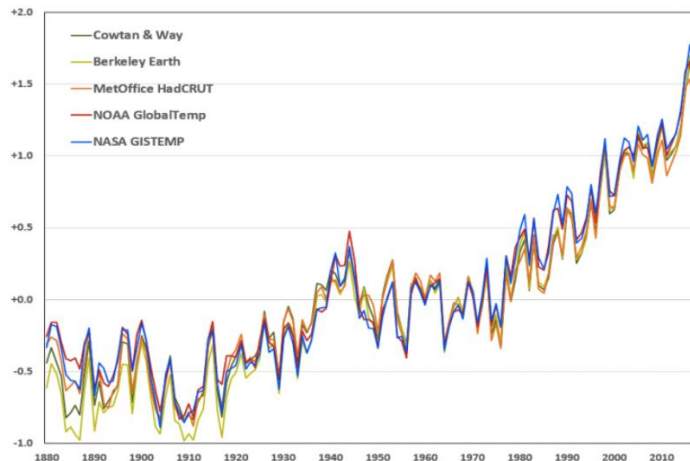


Figure 2.1 *Global temperatures (ww.nasa.gov)*

Ice melting is strongly related to the sea surface temperatures in the Arctic and Antarctic regions. **Figure 2.2** shows the global distribution of sea surface temperatures in May 2001.

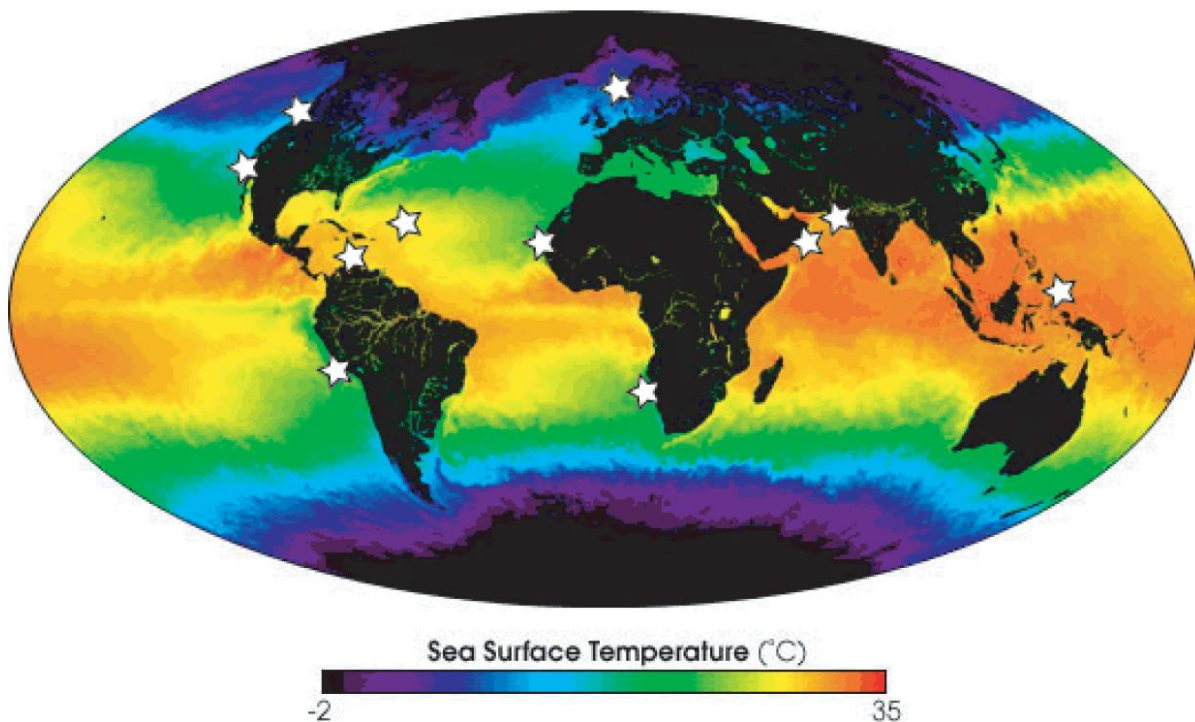


Figure 2.2 *Global sea surface temperatures May 2001 (Modis.gsfc.nasa.gov)*
(white star= marine sediments with interannual to centennial temperature resolution)



The oceans cover over 70% of the Earth's surface and influence climate on a global scale. Heat exchange between the ocean's surface and the atmosphere is crucial to both oceanic and atmospheric circulation patterns. Ocean waters flow from basin to basin driven by differences in water temperature and salinity (and hence density). This is often called the thermohaline 'conveyor belt'. Heat is released to the atmosphere at high latitudes in the North and South Atlantic, where cooling surface waters sink down to form cold, deep water that flows from the Atlantic into the Indian and Pacific Oceans. These deep flows surface again in the northern Indian and Pacific Oceans, to travel back to the Atlantic as warmer, shallow water currents (Thermohaline circulation). On shorter, interannual to decadal timescales, global sea surface temperatures are strongly influenced by atmospheric variability (El Niño effect). Seasonally, sea surface temperatures vary mainly due to changes in the duration and intensity of sunlight (long summer vs. short winter days) as well as storm activity.

Reliable seawater temperature estimates are crucial to any reconstruction and modeling of past ocean salinity and density, water column stratification, thermohaline circulation, and ice volume.

The most commonly used methods to estimate past and future seawater temperatures are as follows:

1. Faunal and floral microfossil assemblages; The abundances and geographic distribution of different marine plankton species are tightly linked to sea surface temperature (SST), and that the percentages of different species contained in a fossil assemblage also reflect the sea surface temperatures they originally lived in.
2. Foraminifer shell chemistry; Marine organisms called foraminifera are single-celled protists that secrete calcium carbonate shells around their cells. The chemistry of these calcite shells provides information about the chemical and physical conditions in which they grew. Foraminifer shells are abundantly found as fossils in marine sediments and thus serve to reconstruct past ocean conditions, particularly surface and deep-sea water temperatures.
3. Alkenone unsaturation index; Organic molecules produced by phytoplankton, namely single-celled, marine algae called coccolithophores produce long-chain, unsaturated methyl and ethyl ketones (alkenones), which can be used to determine SST.

Figure 2.3 shows an example of SST-reconstructions for the past 2000 years.

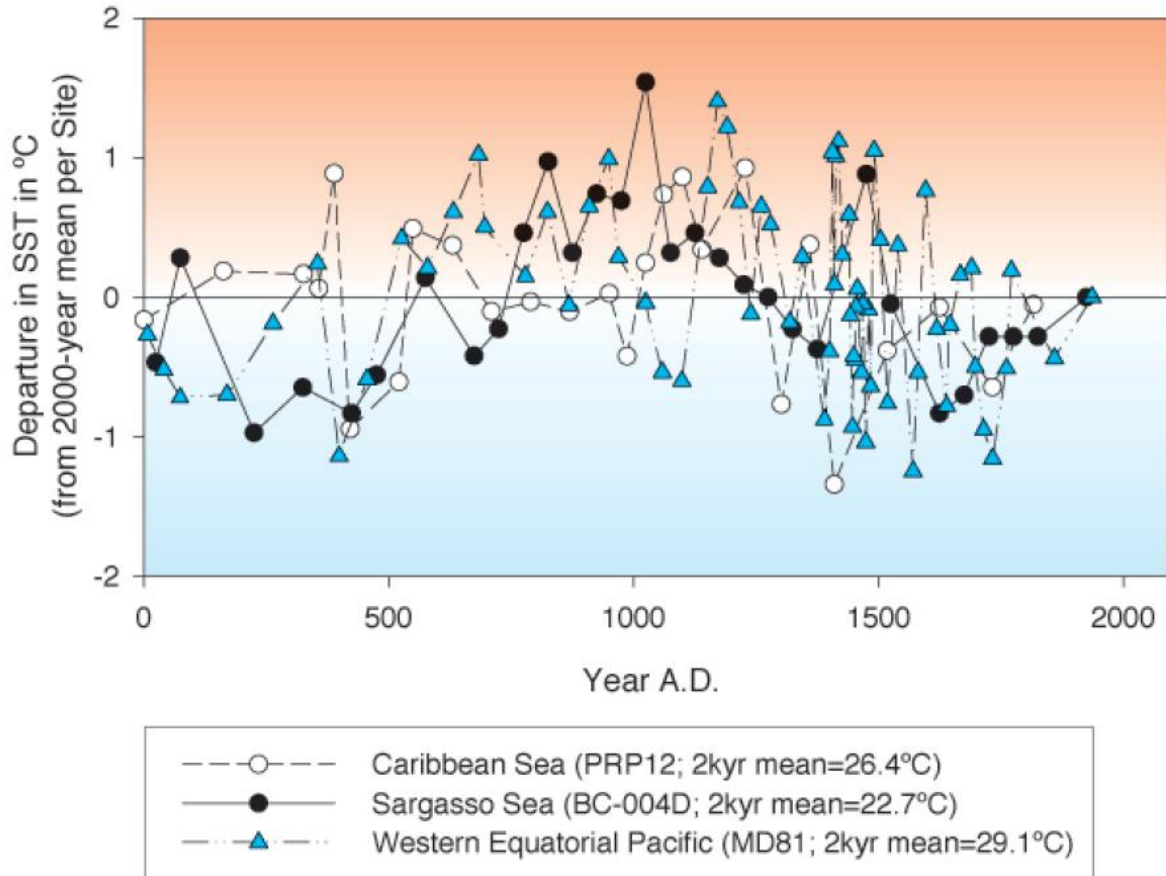


Figure 2.3 Mean sea surface temperature variations for past 2000 years
(Data from Nyberg et al. (2002), Keigwin (1996) and Scott et al. (2004))

Work on decadal to centennial timescales demands a very accurate age control and precise correlation between proxy records. Radiocarbon dating is the most common technique used to date marine sediments, usually carried out on biogenic carbonate (for example planktonic foraminifera) or organic matter. Carbon contained in ocean surface waters is older than the carbon in the atmosphere, the so-called reservoir effect. Therefore, an additional correction needs to be made to convert marine radiocarbon dates to calendar years to enable adequate correlation between various marine records as well as with terrestrial proxy records. In addition, special coring techniques are required to minimize the disturbance of the uppermost centimeters of sediment, which are poorly compacted and therefore easily lost in the coring process.

Temporal resolution of marine sediment records (i.e. how much time is contained within and in what detail) varies greatly due to large regional differences in sedimentation rates and bioturbation. Bioturbation is the mixing of sediments by the burrowing activity of organisms that live at the seafloor, thus averaging out the climatic signals (such as temperature) originally contained in seasonal and annual deposits. Annual and decadal resolution is only acquired in select areas, with rapid, continuous deposition and/or limited bioturbation. Rapid deposition is typically found in highly productive areas, such as upwelling regions off north- and southwest Africa, western South America and the Arabian Peninsula, but bioturbation affects the record.

Centennial to millennial resolution is found in the open marine environment from which we can gain invaluable information on longer-term climate variability, in which the oceans play a crucial and large role.



2.2 Sea surface temperatures (SST) during the last interglacial period (LIG)

During the last interglacial period, between 129,000 and 116,000 years ago (129 ka and 116 ka; ka=1000 years), the global sea levels were 5 to 10 meters higher than at present. During this period, the CO₂ levels were in the range of 250 to 270 ppm, see **Figure 2.4**.

Based on **Figure 2.4**, there is significant correlation between CO₂-level and the temperature change. Roughly: **temperature rises (on the long term) by 10 °C by if CO₂ rises from 200 to 300 ppm.**

Figure 2.4 marks the long term behaviour of CO₂ and temperature variations, but cannot be used to derive the short term influence of CO₂ on temperature variations. Variations of 3 to 5 °C on the shorter term time scale of 5000 years can be observed. The longterm trend cannot be extrapolated linearly to present situation (2018), because the temperature change seems to stagnate while the CO₂-level rises to about 370 ppm, see **Figure 2.4** (year 0).

Scientists have long wondered how global atmospheric and ocean temperatures then compared to modern times, but efforts to reconstruct such temperatures have often fallen short.

In a new study by Hoffman et al. , J. S. Hoffman, P. U. Clark, A. C. Parnell, Feng He. Regional and global sea-surface temperatures during the last interglaciation. *Science*, 2017; 355 (6322): 276 DOI: [10.1126/science.aai8464](https://doi.org/10.1126/science.aai8464)) have revealed that SSTs during the last interglacial were similar to modern day temperatures.

Hoffman et al. compiled 104 published LIG sea surface temperature (SST) records from 83 marine sediment core sites. They compared each core site to data sets from the recent period 1870-1889 and 1995-2014, respectively. Their analysis reveals that, at the onset of the LIG 129,000 years ago, the global ocean SST was already similar to the 1870-1889 average.

However, by 125,000 years ago, the global SST increased by $0.5^{\circ} \pm 0.3^{\circ}$ Celcius, reaching a temperature similar to the average value of the period 1995-2014. These results suggest that LIG global mean annual SSTs simulated with most global climate models are too low. As well, the data show that the Atlantic Ocean in the Northern Hemisphere was cooler at the beginning of the LIG, compared to temperatures in the Southern Hemisphere.

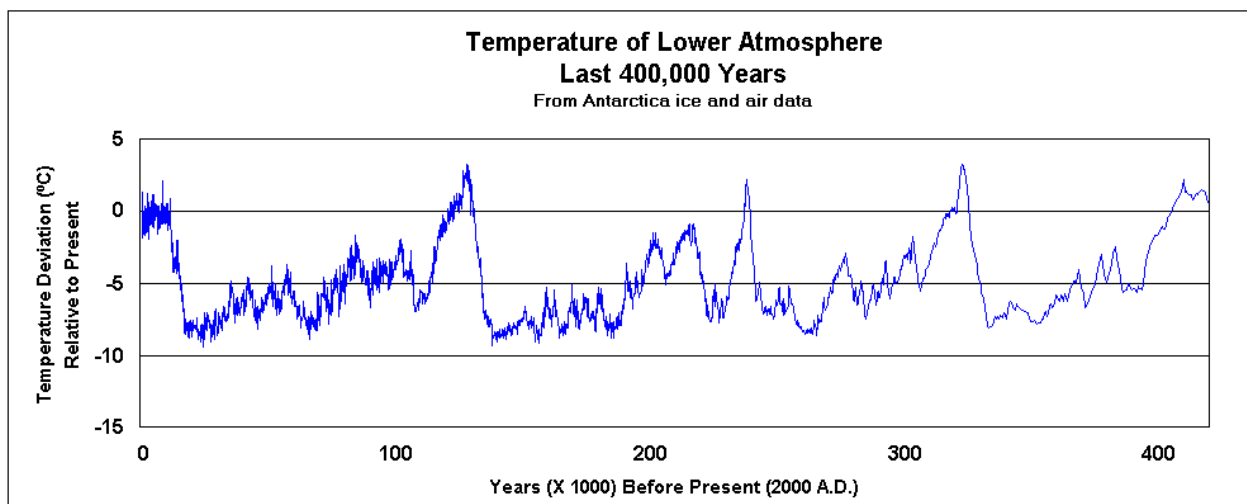
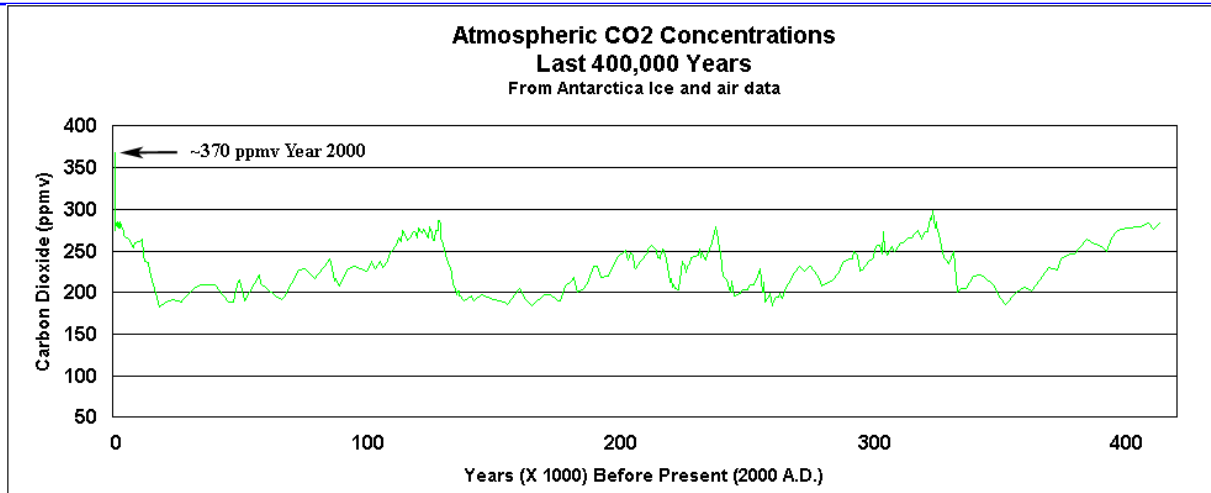


Figure 2.4 CO₂- levels and temperature changes during the last 400,000 years (www.geocraft.com).

Some characteristic data for the last inter glacial period (LIG) and post glacial period (PG) are given in **Table 2.1**. Based on recent Danish research, the last glacial period ended about 12,000 years ago.

Time (years before present)	CO ₂ (ppm)	Temperature to present (°C)	Sea level (m below present)	Mean Sea level rise (mm/year)
129,000-116,000 Last InterGlacial	250-270	0 to +3	5 to 10	≅ 0.4 to 0.8
116,000-12,000 Last Glacial	190-250	-5 to -7	>100	-
12,000-8000 Post Glacial	≅ 250	-7 to -1	>15	> 4
8000-200 Post Glacial	250-300	0 to -1	15 to 0.3	≅ 2
200-present	300-400	1 to -1	0.3 to 0	≅ 1.5

Table 2.1 Sea level rise data of the last 130,000 years (LIG and PG)



3. Ice masses

Most of the ice masses are accumulated on Antarctica and Greenland.

Antarctica

The most striking fact about the Antarctic continent is its almost complete glaciation (ice mountains). The average temperature in Antarctica is -55°C , and the continent covers the entire area from the South Pole to the southern polar circle. Antarctica is a continent of its own and is covered by a massive ice sheet with a thickness of about 5 km in some areas. In addition, Antarctica is surrounded by immense ice fields, which are an enormous network of interconnected valleys with high peaks.

The massive ice desert measures about 15 million km^2 with an ice volume of about 30 million km^3 , see **Table 3.1**.

Arctica

Unlike Antarctica, the Arctic is not a continent which is the predominant different between the two polar regions. Under the massive ice cap of the Arctic lies the Arctic Ocean whose depths reach 5000 m below the surface. Though the Arctic is obviously a very cold region, it is still much warmer than Antarctica in the South. The Arctic region is mainly located in the north polar ocean and includes several larger islands such as Greenland, Spitzbergen, Franz Josef Land, Severnaya Zemlya Wrangel Island, Bank Island, Victoria Island, Ellesmere Island and various others that all border countries like Russia, Canada, Alaska and Greenland. The north polar ocean is covered by permanent ice caps that generally extend far south during the Arctic winter and are made up of around 16 million km^2 of ice.

As the arctic ice is floating (no land ice), the melting of this ice does not contribute to sea level rise.

Greenland (www.dmi.dk)

Ice mass budgets are given on the website www.dmi.dk under Greenland/surface mass budget, see also **Table 3.1**. The total volume of Greenland land ice with dimensions of $1500 \times 1000 \text{ km}^2$ and ice thickness of 2 km is about **3 million km^3** (wikipedia.org).

When snow falls on top of the ice sheet year after year, the layers below are slowly compressed into ice, see **Figure 3.1**. Due to gravity, ice flows slowly outwards. In the central part of the ice sheet, where little if any melt occurs, new layers will therefore continually be added. The ice does not grow in height, however, since the extra ice is balanced by the flow away from the center. Further out towards the coast we find the equilibrium line, where snowfall and melt are exactly balanced. Below the equilibrium line, there is more melt than snowfall and here the net mass loss is countered by the flow coming out from the center of the ice sheet. Here it is the ice sheet itself which melts.

For an ice sheet that neither grows or shrinks, there is at all points averaged over the year a balance between:

- the amount of snow that falls and is compressed to ice;
- the amount of snow and ice that melts or evaporates (sublimates) and;
- the amount of ice that flows away due to the ice motion.

Balance equation: $N_{\text{ice mass}} = G_s - L_{\text{im}} - L_{\text{ic}}$

$N_{\text{ice mass}}$ = net change of ice mass; G_s = mass gain due to snow fall; L_{im} = mass loss due to ice melting; L_{ic} = mass loss due to ice calving into the ocean (icebergs)



When climate changes, the surface mass balance may change such that it no longer matches the calving and the ice sheet can start to gain or lose mass.

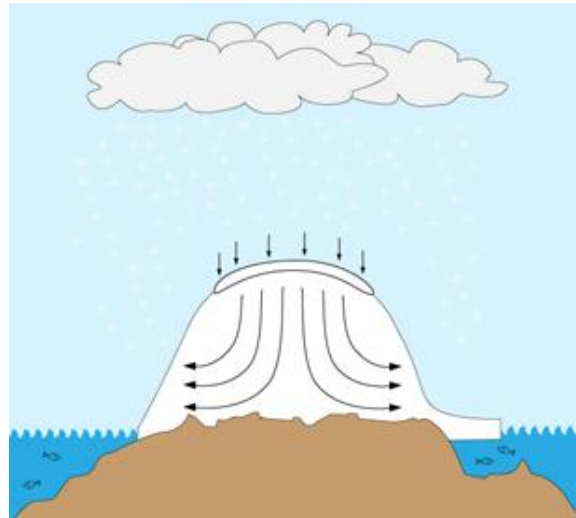


Figure 3.1 *Ice mass balance: Accumulation of snow on top increases mass; Snow is transformed to ice that flows down towards the margins; Melt in lower regions of the ice sheet and iceberg calving from glaciers reduces the mass; If mass loss exceeds mass gain the ice sheet will shrink.*

Type of ice	Surface area of ice (km ²)	Volume of ice above ocean level (km ³)
Antartica	15 10 ⁶	25 10 ⁶
Greenland	1.5 10 ⁶	2.5 10 ⁶
Glaciers (about 200,000)	0.7 10 ⁶	0.15 10 ⁶

Table 3.1 *Ice around the world*

At present the total amount of ice accumulated in Antartica, Greenland and the main glaciers on earth (Alaska, Iceland, Scandinavia, etc) is about **30 million km³** (KMNI, The Netherlands, see www.knmi.nl), see **Table 3.1**.

Figure 3.2 shows the ice sheet of Greenland with area of 1500x1500 km² and thickness of 1 km projected on the map of Europe. The annual ice melt on Greenland is of the order of 300 km³ (see Section 4.4) which is represented as a tiny white block with area of 17x17 km² and thickness of 1 km. It takes about 10,000 years for complete melting of the total ice sheet.



Figure 3.2 Ice sheet with thickness of 1 km and same area as ice sheet on Greenland



4. Ice melting and sea level rise

4.1 General

The melting of ice and related sea level rise can be estimated fairly easily using available data from the Internet, as will be shown hereafter.

Complete melting of all ice leads to sea level rise values, as follows:

- glaciers: 0.5 m (time scale of 0 to 500 years),
- Greenland: 5 m (time scale > 10,000 years),
- Antarctica: 50 m (time scale > 100,000 years).

To compute realistic sea level rise values, the following assumptions are used:

- temperature increase of $\Delta T_{100y} = 3 \text{ }^\circ\text{C}$ over 100 years;
- surface area of oceans of $A_{\text{ocean}} \cong 350 \cdot 10^6 \text{ km}^2$;
- mean depth of oceans of about $h_{\text{ocean}} \cong 5000 \text{ m}$;
- density of ice of about 1000 kg/m^3 (920 kg/m^3 is more realistic value);
- 1 gigaton = 10^9 ton ; $1 \text{ km}^3 = 10^9 \text{ m}^3 \text{ water} = 10^9 \text{ ton water} \cong 0.9 \cdot 10^9 \text{ ton ice}$.

4.2 Thermal expansion of water

The volume increase of the upper water layer over 100 years due to a temperature increase of $3 \text{ }^\circ\text{C}$ is:

$$\Delta V_{100y} = \alpha V_{\text{layer}} \Delta T_{100y}$$

with:

V_{100y} = volume increase over 100 years;

$V_{\text{layer}} = \gamma h_{\text{ocean}} A_{\text{ocean}}$ = volume of water layer experiencing temperature increase;

γ = fraction (0.05-0.15) of water column with higher temperature (layer of 250-750 m);

ΔT_{100y} = temperature increase over 100 years ($= 3 \text{ }^\circ\text{C}$);

α = expansion coefficient of sea water (temperature of $15 \text{ }^\circ\text{C}$) per degree Celsius $\cong 1.5 \cdot 10^{-4} (1/^\circ\text{C})$

The sea level rise over 100 years is

$$\Delta S_{100y} = \Delta V_{100y} / A_{\text{ocean}} = \alpha \gamma h_{\text{ocean}} \Delta T_{100y}$$

Using: $\alpha = 1.5 \cdot 10^{-4}$, $h_{\text{ocean}} = 5000 \text{ m}$, $\gamma = 0.05-0.15$, $\Delta T_{100y} = 3 \text{ }^\circ\text{C}$, it follows that:

$$\Delta S_{100y} = 0.00015 \times (0.05 \text{ to } 0.15) \times 5000 \times 3 \cong 0.1 \text{ to } 0.3 \text{ m for a layer of 250 to 750 m}$$

4.3 Glaciers

Most of the world's glacial ice (about 200,000 glaciers) is found on Antarctica (91%) and Greenland (8%), but glaciers are present on all continents (even Africa). Total ice volumes are given in **Table 3.1**.

The total ice volume of glaciers is about $0.15 \cdot 10^6 \text{ km}^3$, which is equivalent to a sea level rise of $0.15 \cdot 10^6 / 350 \cdot 10^6 \cong 0.0004 \text{ km} \cong 0.4 \text{ m}$ when all glacial ice is melted.



Assuming an annual melting rate of 250 to 500 km³ per year (similar to the observed melting rate of Greenland; estimate of author), the melting time scale is $0.15 \cdot 10^6 / (250 \text{ to } 500) \cong 300 \text{ to } 600$ years. The sea level rise over 100 years is the total sea level rise/time scale = $0.4 / (3 \text{ to } 6) \cong 0.05 \text{ to } 0.15$ m (so almost 40% of the total glacial ice volume in the coming 100 years!!).

4.4 Greenland

The net annual melting rate **observed** in the period 2002 to 2022 is estimated to be about 270 Gigatonnes/year (Gt) or about 300 km³/year, see **Figure 4.1** and data from www.dmi.dk and www.nasa.gov. Long term oscillations can be seen (20 to 40 years). The total quantity of ice on Greenland is 2.5 million km³ (**Table 3.1**). Thus, it will take about $2.5 \cdot 10^6 / 300 \cong 8,000$ years for complete melting of the Greenland land ice.

The net annual ice loss may increase considerably; say up to about 1500 km³/year around 2120. The net annual ice loss in the period 2020-2120 is herein assumed to be in the range of 300 to 1500 km³/year (low emission to high emission scenario). The sea level rise involved is:

$\Delta S_{100y} = M \times N_{\text{years}} / A_{\text{ocean}} = (300 \text{ to } 1500) \times 100 / (350 \cdot 10^6) \cong 0.00009 \text{ to } 0.00045 \text{ km} = 0.09 \text{ to } 0.45 \text{ m}$ over 100 years.

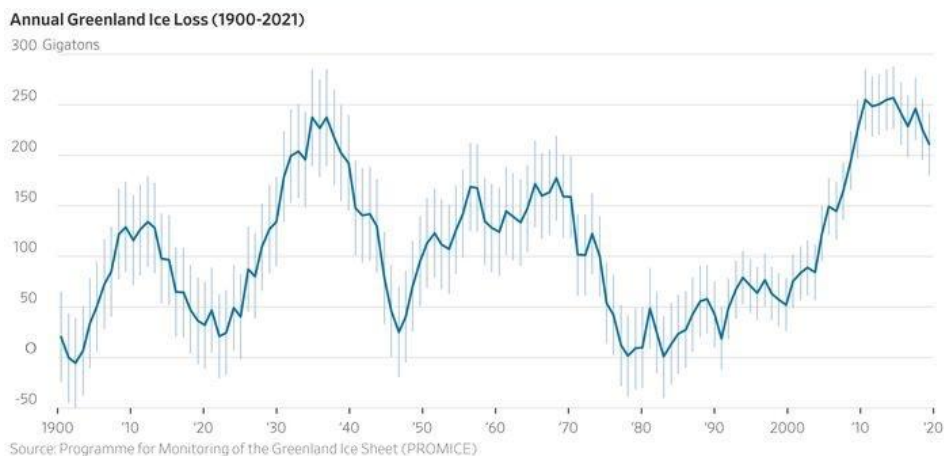
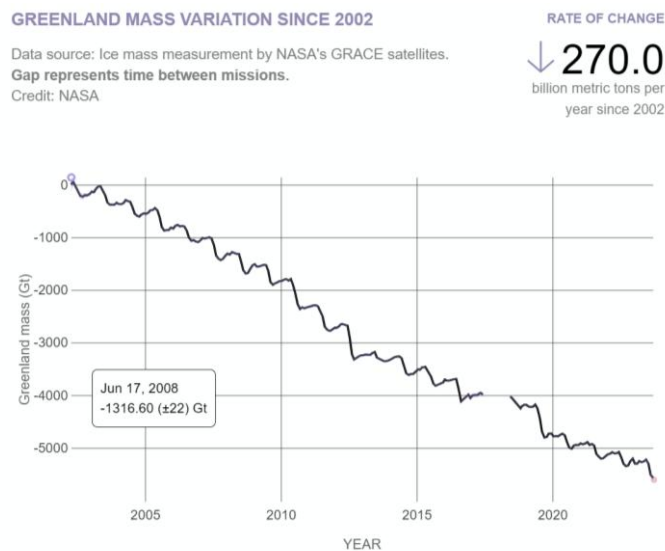


Figure 4.1 *Greenland ice mass variation*
 Upper: since 2002 (Grace satellite data NASA; www.nasa.gov)
 Lower: since 1900 (website: Promice)



Figure 4.2 shows that the snow accumulation on Greenland is increasing since 2010. The values of 300 to 400 Gt in 2019-2021 are higher than the snow melt values of 270 Gt of Figure 4.1. Figure 4.3 shows the total mass balance for Greenland over the period 1986-2020 (Danish Meteorological Institute based on satellite data of GRACE). The ice melt is fairly constant at about 500 Gt/year since 2005. The total mass balance is mostly negative since 2000.

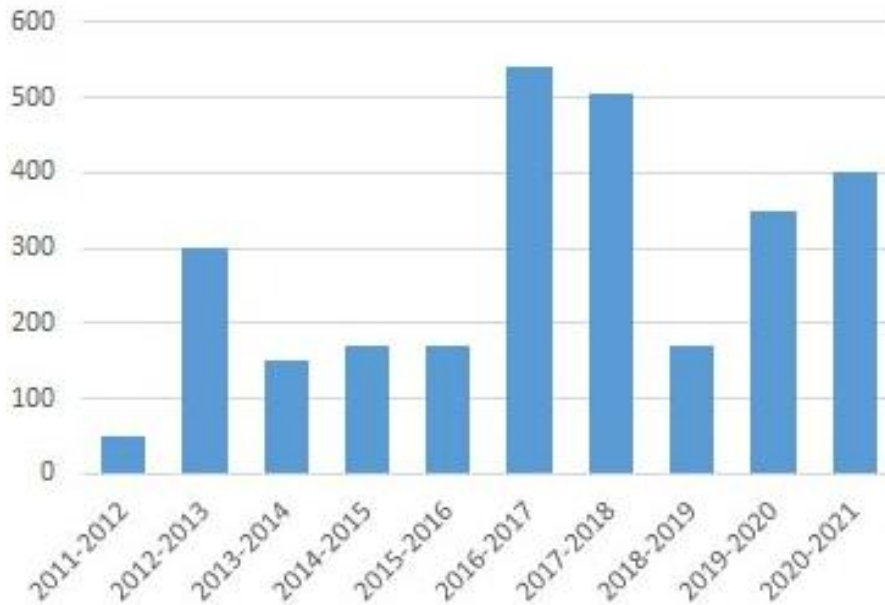


Figure 4.2 Snow accumulation (in Gt) on Greenland since 2010 (source: Polar Portal; klimaatgek.nl)

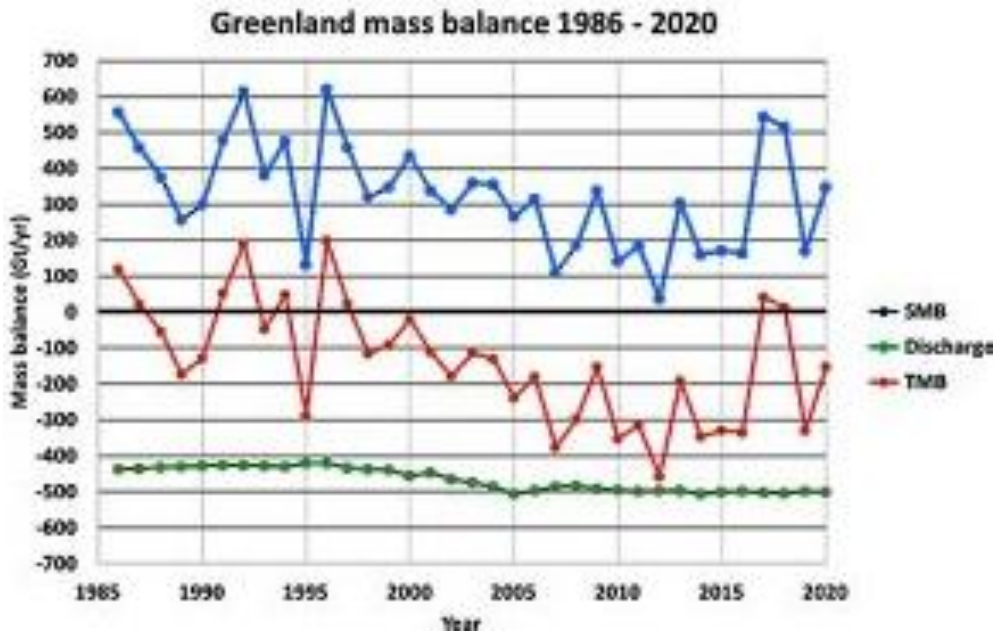


Figure 4.3 Greenland mass balance in GT/year over 1986-2020 (Danish Meteorological Institute) SMB=surface mass change per year; Discharge= Icemelt runoff per year; TMB=total mass change per year



4.5 Antarctica

Snow fall observed

Medley and Thomas (2018) discuss the snowfall on the Antarctic Ice Sheet (AIS). They have reconstructed 200 years (1801-2000) of Antarctic-wide snowfall accumulation by synthesizing a database of ice core records and reanalysis of atmospheric Precipitation minus Evaporation values (P-E values). These latter values are almost equivalent to snow accumulations over the dry, grounded AIS and are more trustworthy over satellite data. Snow accumulation fluctuations are the largest source of uncertainty AIS mass balance estimates. Atmospheric models suggest that snowfall over the AIS will probably rise as atmospheric warming process increases its moisture holding capacity. Significant warming trends over much of Antarctic Peninsula and West AIS (WAIS) hint at the possibility of enhanced snowfall. Ice core records of snow accumulation, the combination of precipitation, sublimation/evaporation and deposition, wind redistribution and melt water runoff fall short of sampling the entire AIS and are noisy due to small scale variability.

Integrated over the entire AIS they observed a clear and significant positive trend in snow accumulation. The snow accumulation in 2000 is about 75 GT (about 75 km³/year equivalent to sea level rise of 0.2 mm; 10% of total present sea level rise of 2 mm/year) larger than the mean value of the period 1800-1900. They have also found that the present increase of snowfall over AIS is related to anthropogenically driven atmospheric circulation changes and warming.

Modern-day accumulation over the AIS is about 80±25 GT/year higher than the mean value of 1801-1900. Snow accumulation at present is estimated to be about one-third (1/3) of the AIS mass loss due to ice melting of about 220±45 GT/year.

Ice melting rates observed

The polar ice sheets grow via snow accumulation and shrink through melting and the production of icebergs. The rate ice melting is more easy to measure than the rate of ice growing due to snowfall and compression.

Snowfall is very difficult to measure over Antarctica, because i) there are very few weather stations in the frozen continent, and most of them are installed along the coastline and ii) satellites have problems in measuring snow deposition from space. Climate models struggle to replicate the total amount of snow that falls over Antarctica each year. So scientists have to rely on ice cores, cylinders of ice drilled from the ice sheet. But the drilling of ice cores is logistically difficult, so they are sparse and do not cover the entire continent.

Researchers (www.nasa.gov; 13 December 2018) reconstructed how much snow fell over the entire Antarctic continent and nearby islands from 1801 to 2000 using 53 ice cores and three atmospheric reanalyzes (climate models informed by satellite observations). It was found that snow accumulation increased over the 20th century by about 1 mm per decade, and that rate more than doubled after 1979. Most likely, this is caused by the increase of snowfall and its distribution pattern over the ice sheet from 1901 to 2000. The warming atmosphere can hold more moisture, combined with changes in the Antarctic circumpolar westerly winds.

The precise net melting rate of Antarctica is unknown at present. The melting of ice may be compensated by increased snowfall.

Prior to 2012, ice was lost at a steady rate of about 100 10⁹ tons per year (based on measured data). Since 2012, the amount of ice loss per year has increased to about 150 10⁹ tons per year, see **Figure 4.4** (www.nasa.gov). This latter value is equivalent to about 150 km³/year (measured data).



Assuming that the net annual ice loss increases from 150 km³/year (in 2020) to **1000 km³/year** around 2120, it follows that:

$$\Delta S_{100y} = M \times N_{\text{years}} / A_{\text{ocean}} = (150 \text{ to } 1000) \times 100 / (350 \times 10^6) \cong 0.00005 \text{ to } 0.0003 \text{ km} = 0.05 \text{ to } 0.3 \text{ m over 100 years.}$$

Most of this loss comes from the huge Pine Island and Thwaites Glaciers on West Antarctica, which are retreating rapidly due to ocean-induced melting.

Based on recent analysis of ice cores, snowfall in Antarctica has increased by 10 per cent since 1800, an analysis of ice cores from Antarctica has revealed. The greatest increase in snowfall has been over the Antarctic Peninsula. It used to be thought that increased snowfall in the Antarctica would more than counter any ice loss due to warming. Early IPCC reports forecast that the ice sheets of Antarctica would grow over the 21 century. As the snow builds up, it is gradually compressed and turned into ice. However, gravity-measuring satellites have shown that the ice sheets of Antarctica have been losing mass since at least 2002.

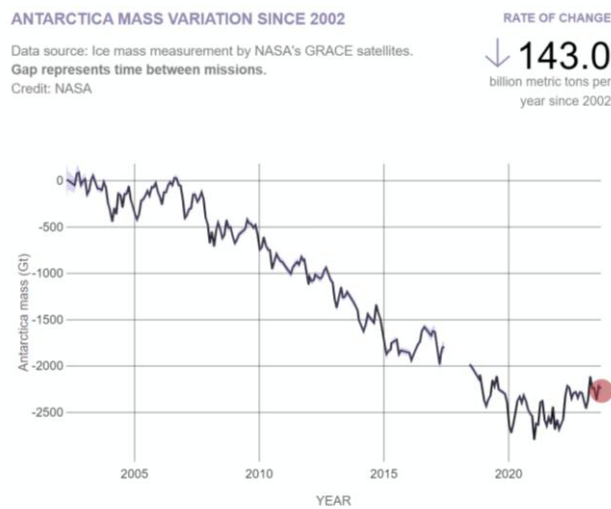


Figure 4.4 Antarctic ice mass variation since 2002 (based on Grace satellite data of NASA)

Recent insights ice melting Antarctica

De Conto and Pollard (Contribution of Antarctica to past and future sea level rise, 2016; Doi: 10.1038/Nature 17145) show that the ice melting at Antarctica may be significantly larger than anticipated up to now, because the Ice cliff dynamics have been neglected in earlier research.

During the more recent Last Interglacial (LIG, 130,000 to 115,000 years ago), the global mean sea level (GMSL) was 6–9.3 m higher than it is today, at a time when atmospheric CO₂ concentrations were below 280 ppm (by volume) and global mean temperatures were only about 0–2 °C warmer. This requires a substantial sea-level contribution from Antarctica of 3.6–7.4 m in addition to an estimated 1.5–2 m from Greenland and around 0.4 m from ocean steric effects (thermal expansion effects). It is difficult to obtain the inferred sea-level values for LIG from ice-sheet models without Ice cliff dynamics included.

Marine ice sheet and ice cliff instabilities; Much of the West Antarctic Ice Sheet (WAIS) sits on bedrock hundreds to thousands of meters below sea level. Despite their thickness (typically about 1 km near the grounding line to a few hundred meters at the calving front), a warming ocean has the potential to quickly erode ice shelves from below, at rates exceeding 10 m yr⁻¹ °C⁻¹. Ice-shelf thinning and reduced backstress enhance seaward ice flow, grounding-zone thinning, and retreat. Because the flux of ice across the grounding line increases strongly as a function of its thickness,



initial retreat onto a reverse-sloping bed (where the bed deepens and the ice thickens upstream) can trigger a runaway Marine Ice Sheet Instability (MISI Fig. 4.5a,b,c).

So far, the potential for MISI to cause ice-sheet retreat has focused on the role of ocean-driven melting of buttressing ice shelves from below. However, it is often overlooked that the major ice shelves in the Ross and Weddell seas and the many smaller shelves and ice tongues buttressing outlet glaciers are also vulnerable to atmospheric warming. Today, summer temperatures approach or just exceed 0 °C on many shelves, and their flat surfaces near sea level mean that little atmospheric warming would be needed to dramatically increase the areal extent of surface melting and summer rainfall.

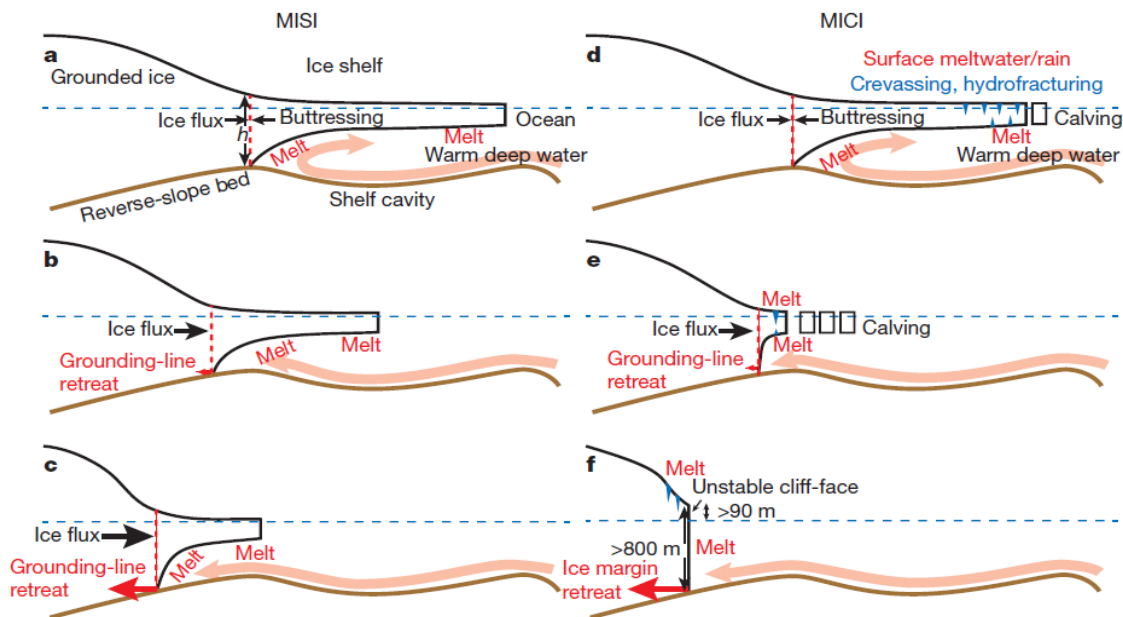


Figure 4.5 MISI and MICI effects (De Conto and Pollard 2016)

- a) Stable, marine-terminating ice-sheet margin, with a buttressing ice shelf. Seaward ice flux is strongly dependent on grounding-line thickness h . Sub-ice melt rates increase with open-ocean warming and warm-water incursions into the ice-shelf cavity.
- b) Thinning shelves and reduced buttressing increase seaward ice flux, backing the grounding line onto reverse-sloping bedrock.
- c) Increasing h with landward grounding-line retreat leads to an increase in ice flow across the grounding line in a positive runaway feedback until the bed slope changes.
- d,e) In addition to MISI (a–c), the model physics used here account for surface-meltwater-enhanced calving via hydrofracturing of floating ice (e), providing an additional mechanism for ice-shelf loss and initial grounding-line retreat into deep basins.
- f) Where oceanic melt and enhanced calving eliminate shelves completely, subaerial cliff faces at the ice margin become structurally unstable where h exceeds 800 m, triggering rapid, unabated MICI retreat into deep basins.

Meltwater on ice-shelf surfaces causes thinning if it percolates through the shelf to the ocean. If refreezing occurs, the ice is warmed, reducing its viscosity and speeding its flow. The presence of rain and meltwater can also influence crevassing and calving rates (hydrofracturing) as witnessed on the Antarctic Peninsula’s Larson B ice shelf during its sudden break-up in 2002. Similar dynamics could have affected the ice sheet during ancient warm intervals, and given enough future warming,



could eventually affect many ice shelves and ice tongues, including the major buttressing shelves in the Ross and Weddell seas.

Another physical mechanism previously underappreciated at the ice-sheet scale involves the mechanical collapse of ice cliffs in places where marine-terminating ice margins approach 1 km in thickness, with >90 m of vertical exposure above sea level. Today, most Antarctic outlet glaciers with deep beds approaching a water depth of 1 km are protected by buttressing ice shelves, with gently sloping surfaces at the grounding line (**Fig. 4.5d**). However, given enough atmospheric warming above or ocean warming below (**Fig. 4.5e**), ice-shelf retreat can outpace its dynamically accelerated seaward flow as buttressing is lost and the few places where such conditions exist today (Helheim and Jakobsavn glaciers on Greenland and the Crane Glacier on the Antarctic Peninsula), hinting that a Marine Ice Cliff Instability (MICI) in addition to MISI could be an important contributor to past and future ice-sheet retreat.

Three-dimensional ice sheet–ice shelf model; The model of De Conto and Pollard (2016) predicts the evolution of continental ice thickness and temperature as a function of ice flow (deformation and sliding) and changes in mass balance via precipitation, runoff, basal melt, oceanic melt under ice shelves and on vertical ice faces, calving, and tidewater ice-cliff failure. The model captures MISI effects by accounting for migrating grounding lines and the buttressing effects of ice shelves with pinning points and side-shear. To capture the dynamics of MICI, new physical treatments of surface-melt and rainwater-enhanced calving (hydrofracturing) and grounding-line ice-cliff dynamics have been added. Including these processes, the model's contributions to Pliocene GMSL and LIG GMSL were found to be in better agreement with available data records.

Model performance; The warm mid-Pliocene and LIG provide complementary targets for model performance, via the ability to produce GMSL values of about 5–20 m (Pliocene) and about 3.5–7.5 m (LIG) from Antarctica, respectively. These two time periods highlight model sensitivities to different processes, because Pliocene summer air temperatures were capable of producing substantial surface meltwater, especially during warm austral summer orbits. Conversely, LIG temperatures were cooler, with limited potential for surface meltwater production. Instead, ocean temperatures could have been the determining factor in LIG ice retreat.

To simulate Pliocene and LIG ice sheets, De Conto and Pollard couple the ice model to a high-resolution, atmospheric regional climate model (RCM) adapted to Antarctica and nested within a global climate model (GCM). The RCM captures the orographic details of ice shelves and adjacent ice-sheet margins, which is critical here because the new calving and grounding line processes are mechanistically linked to the atmosphere. De Conto and Pollard use a modern ocean climatology interpolated to our ice-sheet grid, with uniformly imposed sub-surface ocean warming providing melt rates on sub-ice-shelf and calving-front surfaces exposed to sea water. The RCM climatologies and imposed ocean warming are applied to quasi-equilibrated initial ice-sheet states, with atmospheric temperatures and the precipitation lapse-rate corrected as the ice sheet evolves.

The Pliocene simulation uses a RCM climatology with 400 ppm CO₂, a warm austral summer orbit, and 2 °C imposed ocean warming to represent maximum mid-Pliocene warmth. The model produces an 11.3-m contribution to GMSL rise. Pliocene retreat is triggered by meltwater-induced hydrofracturing of ice shelves, which relieves backstress and initiates both MISI and MICI retreat into the deepest sectors of West and East Antarctic Ice Sheets (WAIS and EAIS) marine basins.



The LIG-simulation is based on summer air temperatures in the RCM which are slightly warmer at 116 kyear ago than 128 kyear ago, but remain below freezing in both cases, with little to no surface. As a result, substantial oceanic warming $>4\text{ }^{\circ}\text{C}$ is required to initiate WAIS retreat at 128 kyear ago, which occurs once an ocean-melt threshold is reached in the stability of the Thwaites grounding line. Allowing two-way coupling between the RCM and the ice-sheet model captures dynamical atmospheric feedbacks as the ice margin retreats. This enhances retreat, but still requires $>4\text{ }^{\circ}\text{C}$ of ocean warming to produce a $>3.5\text{ m}$ increase in GMSL. De Conto and Pollard find that by accounting for the additional influence of circum-Antarctic ocean warming on the RCM atmosphere, the GMSL contribution increases to $>6.5\text{ m}$ with **just $3\text{ }^{\circ}\text{C}$ sub-surface ocean warming**, despite the cooler orbit of the Earth 128 kyear ago. The ocean-driven continental warming at 128 kyear ago agrees with ice core records and supports a Southern Ocean control on the timing of ice-sheet retreat, possibly through Northern Hemisphere influences on the ocean meridional overturning circulation.

Alternative simulations use time-evolving atmospheric and oceanic climatologies based on marine and ice-core proxy reconstructions. These time-continuous simulations produce GMSL contributions of 6–7.5 m early in the interglacial, followed by a prolonged plateau and rapid recovery of the ice sheet beginning around 115 kyear ago. This result matches the magnitude, temporal pattern, and rate of LIG sea-level change, and the simulated recovery of the WAIS satisfies the presence of ice >70 kyear ago at the bottom of the WAIS Divide Ice Core.

Combined with estimates of Greenland ice loss and ocean thermal effects, the simulated, Antarctic contributions to Pliocene and LIG sea level are in much better agreement with geological estimates than previous versions of our model, which lacked these new treatments of meltwater-enhanced calving and ice-margin dynamics, suggesting that the new model is better suited to simulations of future ice response.

Long term effects: Ocean warming alone may be limited in its potential to trigger massive, widespread ice loss, but the multi-millennial thermal response time of the ocean will have a profound influence on the ice sheet's recovery. In simulations run 5,000 years into the future, we conservatively assume no ocean warming beyond 2300 and simply maintain those ocean temperatures while the atmosphere cools assuming different scenarios of CO_2 drawdown beginning in 2500. For RCP8.5 and natural CO_2 drawdown, GMSL continues to rise until 3500 with a peak of about 20 m, after which the warm ocean inhibits the re-advance of grounding lines into deep marine basins for thousands of years. Even in the moderate RCP4.5 scenario with rapidly declining CO_2 after 2500, WAIS is unable to recover until the global ocean cools, implying a multi-millennial commitment to several meters of sea-level rise despite human-engineered CO_2 drawdown.

Given uncertainties in model initial conditions, simplified hybrid ice dynamics, parameterized sub-ice melt, calving, structural ice-margin failure, and the ancient sea-level estimates used in the Large Ensemble analysis, the rates of ice loss simulated here should not be viewed as actual predictions, but rather as possible envelopes of behaviour that include processes not previously considered at the continental scale. These are among the first continental-scale simulations with model physics constrained by ancient sea-level estimates, simultaneously accounting for high-resolution atmosphere–ice sheet coupling and ocean model temperatures.

However, several important processes are lacking and should be included in future work. In particular, the model lacks two-way coupling between the ice sheet and the ocean. Rapid calving and ice-margin collapse also implies ice mélange in restricted embayments that could provide buttressing and a negative feedback on retreat. The loss of ice mass would also have a strong effect on relative sea level at the margin owing to gravitational and solid-earth deformation effects which could affect MISI and MICI dynamics because of their strong dependency on bathymetry. Future



simulations should include coupling with Earth models that account for these processes. Improved ancient sea-level estimates are also needed to further constrain model physics and to reduce uncertainties in future RCP scenarios.

Despite these limitations, the new model physics are shown to be capable of simulating two very different ancient sea-level events: the LIG, driven primarily by ocean warming and MISI dynamics, and the warmer Pliocene, in which surface meltwater and MICI dynamics are also important.

When applied to future scenarios with high greenhouse gas emissions, the palaeo-filtered model ensembles show the potential for Antarctica to contribute >1 m of GMSL rise by the end of this century, and >15 m meters of GMSL rise in the next 500 years, see **Figure 4.6**.

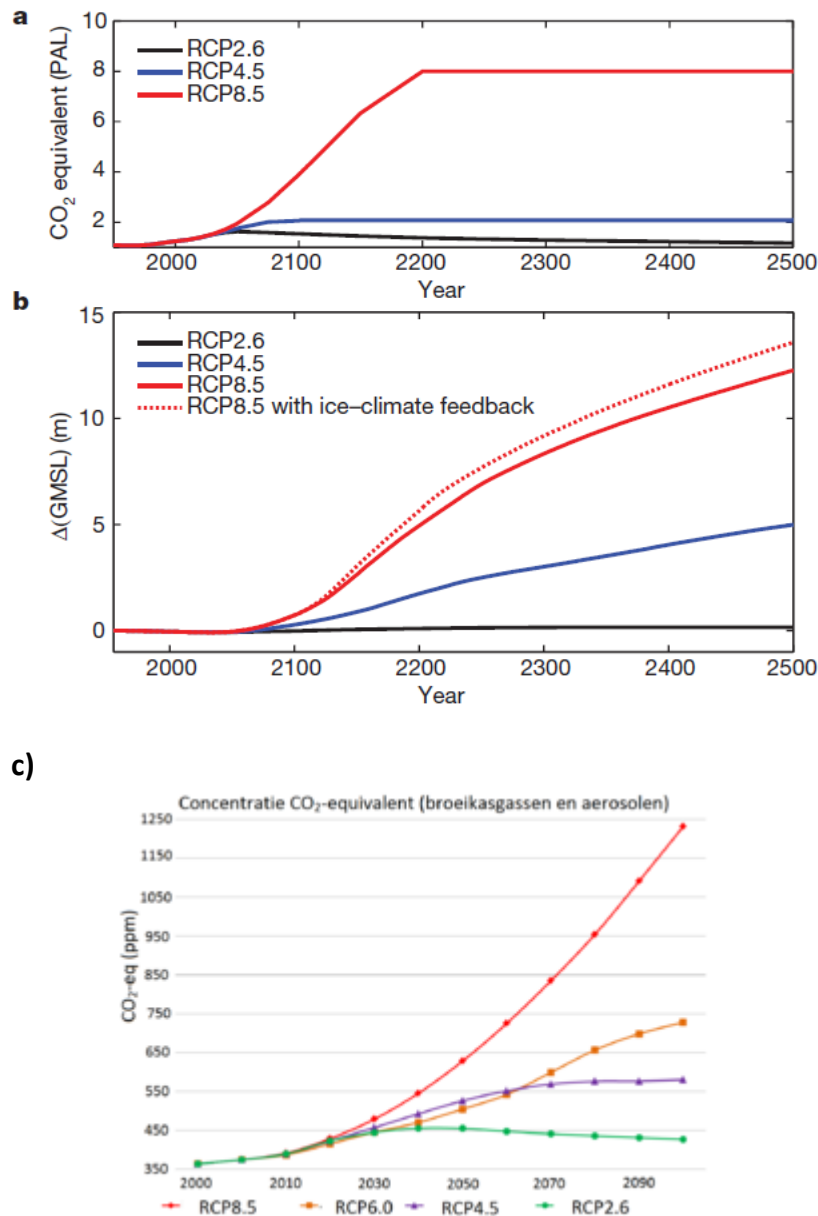


Figure 4.6 Sea level rise contribution due to MISI and MICI effects (De Conto and Pollard 2016)
a) Equivalent CO₂ forcing applied to the simulations (RCP emission scenarios)
b) Antarctic contribution to Global Mean Sea level rise.
c) RCP scenarios (RCP2.6: CO₂< 450 ppm; RCP4.5: CO₂<570 ppm; RCP8.5: CO₂ <1200 ppm)



Morlighem et al. (2024) have studied the collapse of ice shelves at West Antarctic. The collapse of ice shelves could expose tall ice cliffs at ice sheet margins. The marine ice cliff instability (MICI) is a hypothesis that predicts that, if these cliffs are tall enough, ice may fail structurally leading to self-sustained retreat. To date, simulations that include MICI have been performed by Morlighem et al., (2024) with a single model based on a simple parameterization method. They have implemented a physically-based parameterization in three ice sheet models and simulate the response of the Amundsen Sea Embayment after a hypothetical collapse of floating ice. All their models show that the Thwaites Glacier (**Figure 4.7**) would not retreat further in the 21st century. In another set of simulations, they have forced the grounding line to retreat into the 'Thwaites' deeper basin to expose a taller cliff. In these simulations, various processes reduce the calving rate, stabilizing the cliff. These experiments show that the tall Thwaites ice front may be less vulnerable to MICI than previously thought, and model simulations that include this process should be re-evaluated. If this all is true, the most pessimistic scenarios of future sea level rise (1.6 m in 2100 and 15 m in 2300 based on last IPCC-report in March 2023; 2.5 m in 2100 and 17 m in 2300 based on Dutch KMNI report) should be re-evaluated.

The threat from Thwaites: The retreat of Antarctica's riskiest glacier

Ice sheet's demise poses the biggest threat for sea-level rise this century



Figure 4.7 *Thwaites glacier, West-Antarctica*

Andreasen et al. (2023) have studied the growth and retreat of Antarctic ice shelves, see **Figure 4.8**. They have used MODIS (Moderate Resolution Imaging Spectro-radiometer) satellite data to measure the change in ice shelf calving front position and area on 34 ice shelves in Antarctica from 2009 to 2019.

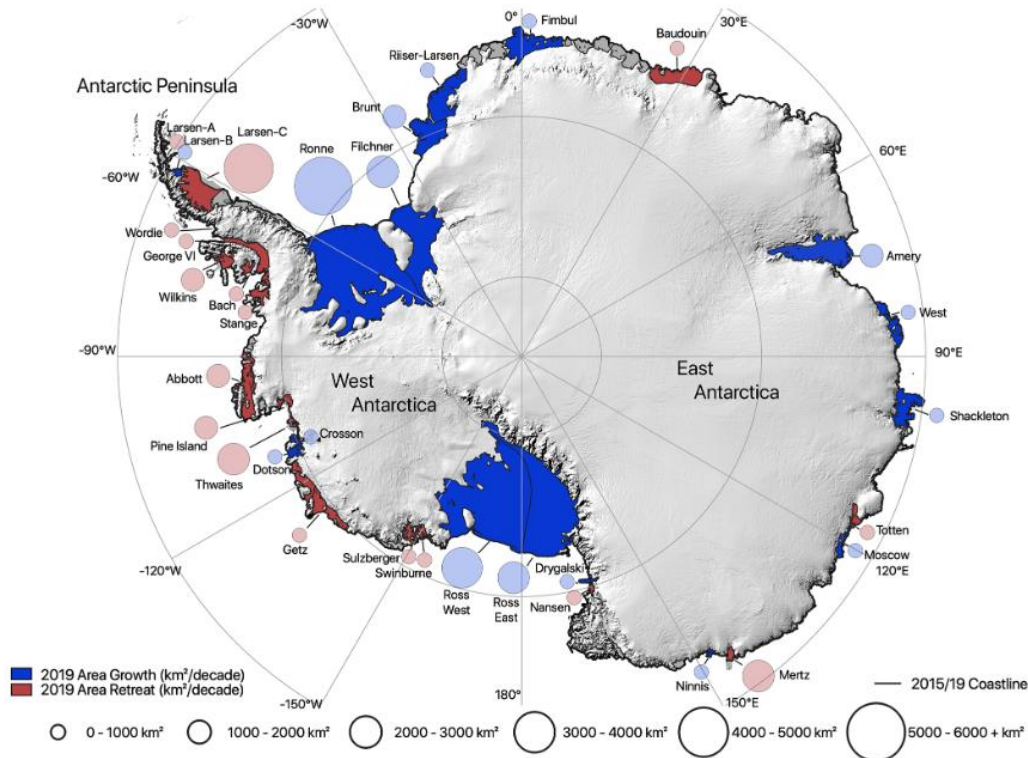


Figure 4.8 Antarctic map of ice shelf area change from 2009 to 2019, with ice shelf names overlaid on a Bedmap2 surface of Antarctica. The circle areas denote the total amount of ice shelf area (in km²) lost (red) or gained (blue). The bold black line represents the Antarctic coastline, combining 2015 and 2019 data.

Over the last decade, a reduction in the area on the Antarctic Peninsula (6693 km²) and West Antarctica (5563 km²) has been outweighed by area growth in East Antarctica (3532 km²) and the large Ross and Ronne–Filchner ice shelves (14 028 km²). The largest retreat was observed on the Larsen C Ice Shelf, where 5917 km² of ice was lost during an individual calving event in 2017, and the largest area increase was observed on Ronne Ice Shelf in East Antarctica, where a gradual advance over the past decade (535 km²/year) led to a 5889 km² area gain from 2009 to 2019. Overall, the Antarctic ice shelf area has **grown** by 5305 km² since 2009, with 18 ice shelves retreating and 16 larger shelves growing in area. Their observations show that Antarctic ice shelves gained 661 Gt of ice mass over the past decade, whereas the steady-state approach would estimate substantial ice loss over the same period, demonstrating the importance of using time-variable calving flux observations to measure change.



4.6 Total sea level rise

Based on all contributions, the total sea level rise over 100 years (2020 to 2120) is estimated by the author (Van Rijn):

Thermal expansion: $\Delta S_{100y} = 0.10$ to 0.30 m

Glaciers: $\Delta S_{100y} = 0.05$ to 0.15 m

Greenland: $\Delta S_{100y} = 0.10$ to 0.45 m

Antartica: $\Delta S_{100y} = 0.05$ to 0.3 m (MISI-effect) to 1.0 m (including MISI+MICI effects)

Total $\Delta S_{100y} = 0.3$ m to 1.2 m $\cong 0.75$ m ± 0.45 m (7.5 ± 4.5 mm/year; no MICI-effect)

Most of the uncertainty is related to the uncertainty of the increased snow fall rate on Antarctica and Greenland and the type of ice melting (MICI-effect).

IPPC report 2022 predicts a sea level rise for this century (up to 2100) between 0.3 and 1.0 m based on 2 RCP-scenarios for concentration (CO_2) emissions, see **Figure 4.9** and **Table 4.1**.

The present (2023) sea level rise is about 3 mm/year (or 0.3 m over 100 years).

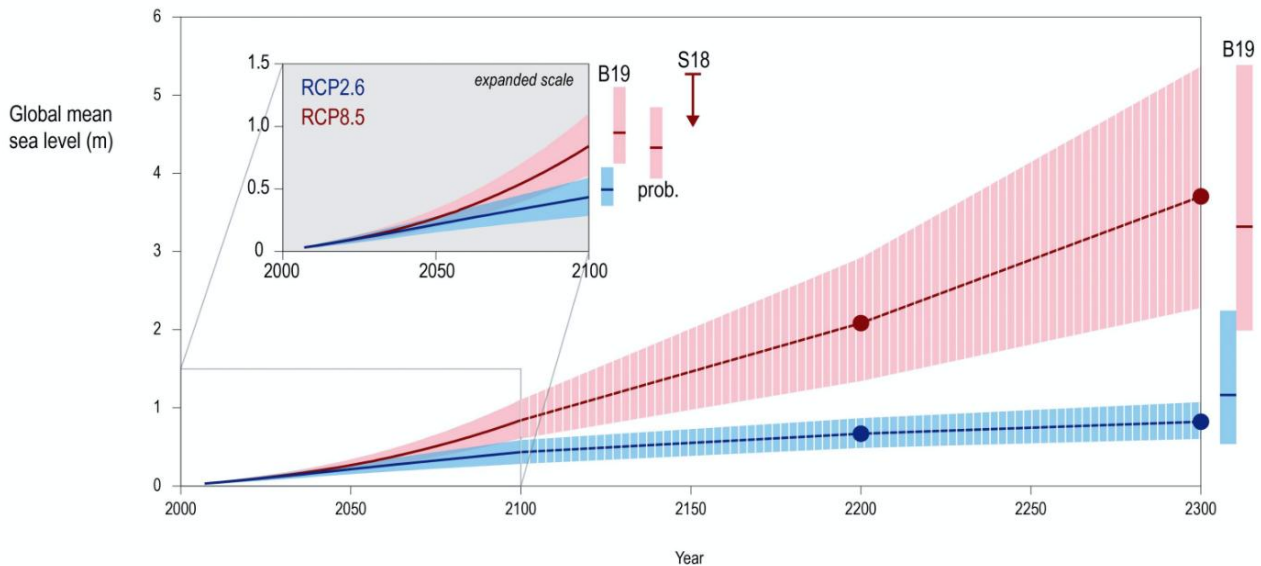


Figure 4.9 Sea level rise values given (IPCC 2022)

Source	1901–1990	1970–2015	1993–2015	2006–2015
<i>Observed contribution to GMSL rise</i>				
Thermal expansion		0.89 (0.84–0.94) ^a	1.36 (0.96–1.76) ^a	1.40 (1.08–1.72) ^a
Glaciers except in Greenland and Antarctica	0.49 (0.34–0.64) ^b	0.46 (0.21–0.72) ^c	0.56 (0.34–0.78) ^p	0.61 (0.53–0.69) ^q
GIS including peripheral glaciers	0.40 (0.23–0.57) ^c		0.46 (0.21–0.71) ^d	0.77 (0.72–0.82) ^d
Antarctica ice sheet including peripheral glaciers			0.29 (0.11–0.47) ^e	0.43 (0.34–0.52) ^e
Land water storage	–0.12 ^f	–0.07 ^f	0.09 ^f	–0.21 (–0.36–0.06) ^g
Ocean mass				2.23 (2.07–2.39) ^h
Total contributions			2.76 (2.21–3.31)^j	3.00 (2.62–3.38)^j
Observed GMSL rise from tide gauges and altimetry	1.38 (0.81–1.95)	2.06 (1.77–2.34)^j	3.16 (2.79–3.53)^k	3.58 (3.10–4.06)^k
<i>Modelled contributions to GMSL rise</i>				
Thermal expansion	0.32 (0.04–0.60)	0.97 (0.45–1.48)	1.48 (0.86–2.11)	1.52 (0.96–2.09)
Glaciers	0.53 (0.38–0.68)	0.73 (0.50–0.95)	0.99 (0.60–1.38)	1.10 (0.64–1.56)
Greenland SMB	–0.02 (–0.05–0.02)	0.03 (–0.01–0.07)	0.08 (–0.01–0.16)	0.12 (–0.02–0.26)
Total including land water storage and ice discharge ^l	0.71 (0.39–1.03)	1.88 (1.31–2.45)	3.13 (2.38–3.88)	3.54 (2.79–4.29)
Residual with respect to observed GMSL rise ^m	0.67 (0.02–1.32)	0.18 (–0.46–0.82)	0.03 (–0.81–0.87)	0.04 (–0.85–0.93)

Table 4.1 Sea level rise (in mm/year) due to contributing processes (IPCC2022)



5. What can we do about Sea Level Rise?

Accelerated Sea Level Rise on short term time scale due to human interference (global warming) is a direct threat to low-lying countries bordering the seas and oceans.

Mitigating measures are (Deltares 2007, 2018; see also **Figure 5.1**):

- construction of (new) higher and wider barriers, dunes and dikes along the coast and lower river sections (defend);
- elevation of existing land surface by large-scale sand suppletion to outraise Sea Level Rise;
- evacuation of the low-lying areas (retreat).

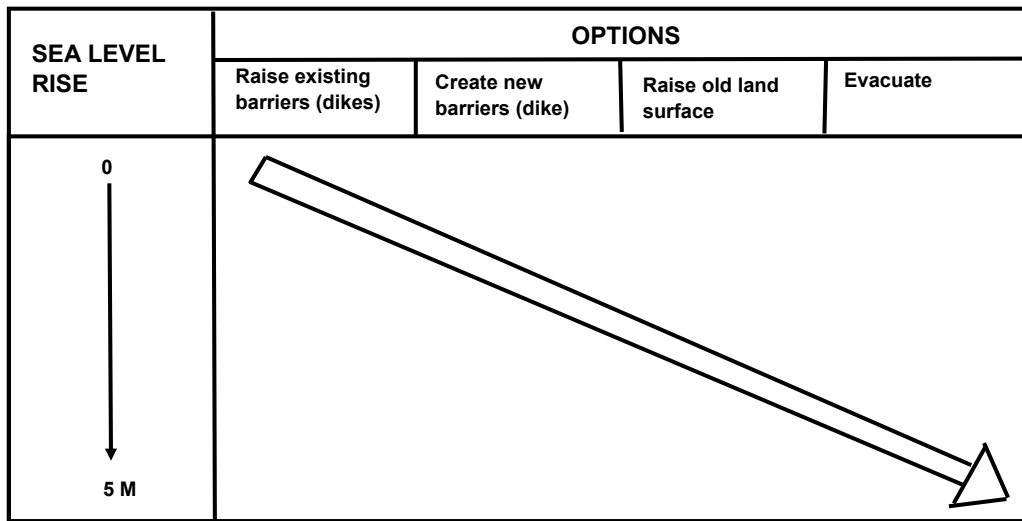


Figure 5.1 Sea Level Rise and counter measures (options)

The primary Dutch coastal defence system consists of (**Figure 5.1**):

- natural sand dunes and artificial sea dikes along the coasts of
 - Holland and Zeeland (\cong 300 km);
 - Friesland and Groningen (\cong 200 km);
 - Wadden islands (\cong 250 km);
 - Westerschelde estuary (\cong 150 km);
- storm surge barriers in the mouths of the Rotterdam Waterway (Maeslant barrier) and the Oosterschelde-estuary.

Furthermore, the dikes along the sea-dominated Rhine branches (\cong 650 km) and along the Oosterschelde-estuary (\cong 150 km) are a crucial part of the inland defence system. In conditions with increased sea level rise and open barriers, the tide will propagate farther inland (larger water depths) and the inland dike system will be under more intensive loading.

Increased sea level rise has a strong effect on the:

- sand nourishment volumes to maintain the coastal zone (beaches and surf zone);
- sand dune dimensions (crest level and dune width);
- sea dike dimensions (crest level and dike width);
- barrier dimensions and closure frequency.



Figure 5.1 Primary coastal defence system, The Netherlands

Deltares (2018) has performed an exploratory study to determine the effects of increased sea level rise on the required sand nourishment volume to maintain the Dutch coastal zone (about 4000 km² excluding Wadden Sea) and the required closure frequency of the existing barriers, see **Table 5.1**. A crude estimate of the required sand nourishment volume can be obtained by multiplication of the nearshore area and the sea level rise value. Higher nourishment volumes are technically feasible as sufficient quantities of sand are available in the Dutch sector of the North Sea. Sand nourishment in the Wadden sea is also required if the rate of sea level rise is larger than about 5 to 6 mm/year; otherwise the tidal flats will gradually drown.

The existing barriers in the Oosterschelde estuary and in the Rotterdam Waterway will be more or less permanently closed when the sea level rise is about 1.5 to 2 m (**Table 5.1**).

Finally, the international dimension of the problem should be realized. In north-west Europe, many countries are threatened by sea level rise: NW-France, Belgium, Netherlands, Germany, Denmark and all countries around Baltic Sea. The total economic value of housing and infra-structure is of the order of 100,000 billion Euro.



Sea level rise	Closure frequency		Sand nourishment volume (for area of 4000 km ² ; excl. Wadden Sea)
	Maeslant barrier Rotterdam Waterway	Oosterschelde barrier	
0.5 m	0.5x per year	7x per year	2 10 ⁹ m ³
1.0 m	5x per year	50x per year	4 10 ⁹ m ³
1.5 m	30x per year	>360x per year	6 10 ⁹ m ³

Table 5.1 Closure frequency of existing barriers and sand nourishment volumes for three sea level rise values (based on Deltares 2018)

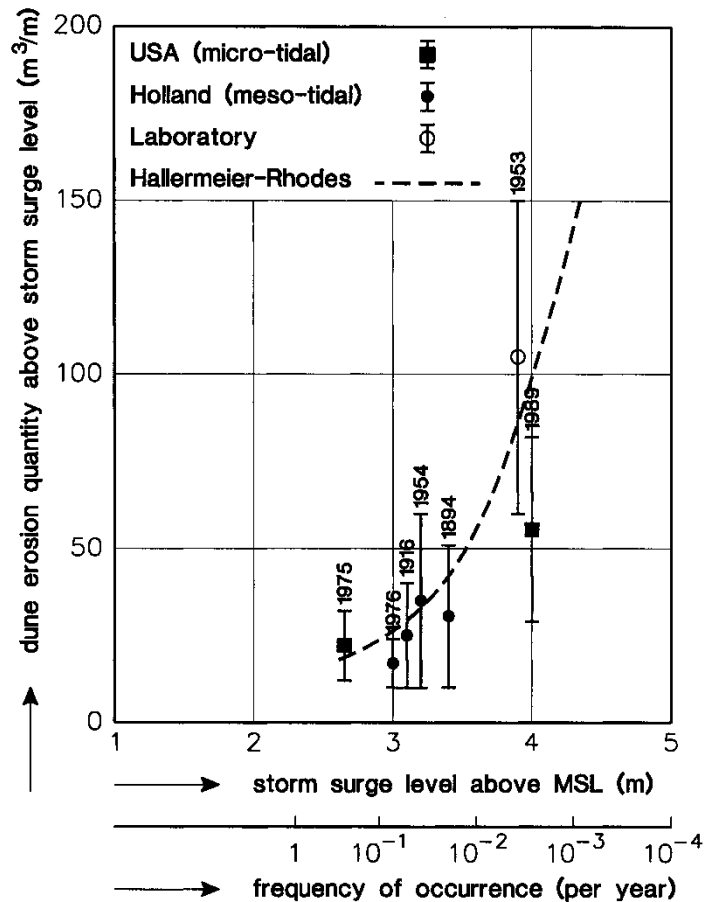


Figure 5.2 Dune erosion volume as function of storm surge level (Vellinga, 1986)

Limited Sea level Rise < 1.5 m

As long as sea level rise remains smaller than about 1.5 m, the most realistic option is to strengthen the existing dune and dike systems along the coasts and along the inland river banks.

The maximum storm surge level during a superstorm in the North Sea is of the order of +8 m above mean sea level (sea level rise of 1.5 m, flood tide level of 1.5 m, wind setup of 4 m). Based on this, the minimum required crest level of dunes and dikes is of the order of +15 m above mean sea level. The maximum dune erosion volume of a natural sand dune facing the sea during a superstorm (assuming an increased wave climate) is of the order of 200 to 300 m³/m above storm surge level (Vellinga, 1986; see **Figure 5.2**) resulting in a dune base width of the order of 100 m.



When open rivers are present, the sea penetrates into the lower river reaches over considerable distance due to tidal flow (flood and ebb). The tidal penetration length increases for higher sea levels. Hence, the dikes in the lower river sections will also be affected by sea level rise. Furthermore, global warming may also lead to increased river discharges (increased rainfall).

Sea level rise > 1.5 m

In the case of excessive sea level rise exceeding 1.5 m, one may consider three very drastic and expensive options:

- elevation of parts of the land surface by large-scale suppletion of sand (assuming that sufficient quantities of sea sand are available);
- strengthening of the primary defence system by raising dunes and dikes; construction of permanent barriers in Rotterdam Waterway and Oosterschelde-estuary (crest levels should be raised by about 5 m); construction of new barrier in Westerschelde estuary;
- construction of a new massive offshore sea dike.

Elevation of land surface

To raise a square kilometer of land by a layer of sand with a thickness of 10 m, a volume of 10 million m³ of sand is required at a price of 30 to 50 millions of Euros depending on the availability and transportation distance of sand. Furthermore, the infrastructure of the old land has to be rebuilt completely in the case of land raising. On the scale of The Netherlands it would mean that a total area about 50,000 km² of the western part of the country has to be raised by 10 m at a price of about 2,500 billion euros. The annual construction costs of this option (about 2 to 3 billion euros per year) are still feasible considering the time scale of 1000 years.

Strengthening of existing primary dunes, dikes and barriers

The complete strengthening of the primary defense system along the coasts of Holland, Zeeland, Friesland, Groningen and the Wadden islands involves the construction of higher and wider dunes and dikes and the construction of permanent barriers in Rotterdam Waterway, Oosterschelde estuary and Westerschelde estuary (crest levels should be raised by about 5 m).

The Oosterschelde barrier has to be replaced by a permanent sea dike. An alternative solution is to raise all dikes along the Oosterschelde estuary. In the latter case the barrier at the mouth loses its function and the movable gates can be removed.

The Maeslant barrier in the Rotterdam Waterway has to be replaced by a permanent closure structure consisting of a seasluice-complex in combination with a large pumping facility to pump out the rhine discharge (mean value of about 1500 m³/s and maximum value of 15.000 m³/s). The scale of this structure requires the design of an extensive nearshore reservoir, see **Figure 5.3**.

A new barrier has to be built in the mouth or at the end of the Westerschelde estuary.

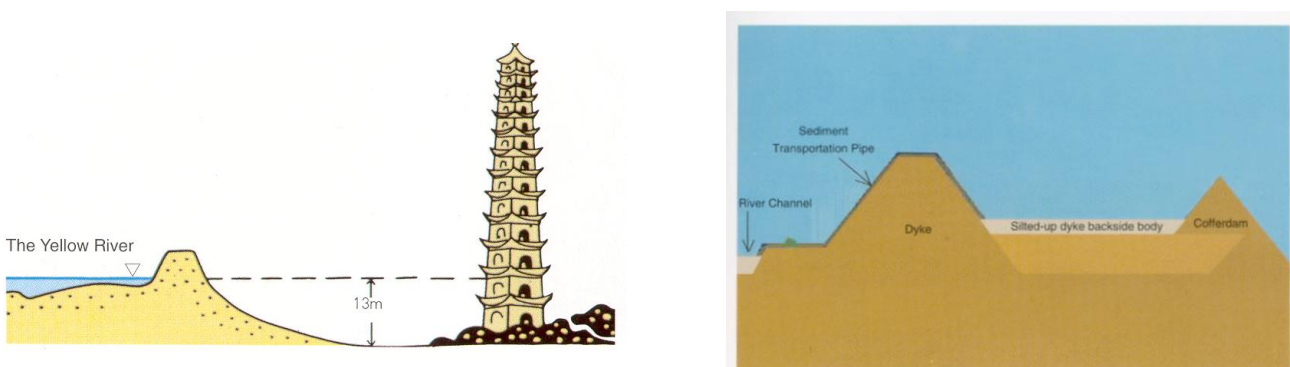


Figure 5.3 Sea sluice complex in Rotterdam Waterway, The Netherlands

The construction of massive dikes is technically feasible. China has shown that the major river flood discharges of the Yellow River can be regulated by a system of massive dikes with a base width of the order of 100 m (Practice of Yellow River Control, Yellow River Conservancy Press, 2004), see **Figure 5.4**. The annual sedimentation in the lower Yellow River is so large that the dike levels have to be raised every 20 years ('hanging' river system with the river bed above the surrounding terrain).

The construction costs of massive dunes and dikes are of the order of 20 millions euros per kilometer. The overall costs will be large (30 billion euros) when the dikes and dunes over a total length of 1500 km have to be strengthened. However, the annual construction costs are not very high (about 1 to 2 billion euros per year) for the Dutch economy, given the time scale of about 20 to 30 years.

The construction costs of three new barriers are of the order 50 billion euros or about 2 to 3 billion euros given a construction period of 20 to 30 years.



Figuur 5.4 Dikes in China (Yellow River Conservancy Press, 2004)

Left: yellow River near Kaifeng

Right: Schematised dike



Offshore sea dike

A rather drastic long-term option for the Northwestern Europe would be the construction of a massive offshore sea dike at the -20 m sea depth contour (base width of 1000 m, crest width of 200 m; height of 50 m, crest at +30 m; length of about 800 km; see **Figure 5.5**) to protect the coastline between France and Norway/Sweden. This requires 20 billion m³ of sand (20,000 million m³). The overall costs (including sluices for shipping, pumping facilities, wind turbines for electricity) are of the order of 10,000 billion (10¹⁰) euros, which is still feasible/acceptable because the construction costs can be spread over a construction period of say 100 years and several countries resulting in an annual investment of around of 10 billion euro per country per year. This latter value is low compared to the annual GDP (Gross Domestic Product) of the countries involved. For example, the annual GDP of the Netherlands is 1000 billion euro per year. The construction costs are low compared to the total value of building and infra-structure in NW-Europe (100,000 billion Euro).

The area inshore of the sea dike will become a large fresh water lake (**Rhine lake**) due to the input of river water. The total pumping capacity to deal with river water input and seepage flows through/under the dike may be as large as 100,000 m³/s requiring a continuous energy input of about 30,000 Megawatt (energy required to raise 1 m³ of water per sec over a vertical distance of 10 m is about 0.3 megawatt).

The scale of such a project requires an international cooperation between France, Belgium, The Netherlands, Germany, Denmark, Norway, Sweden, Poland to construct a new defense line between the high cliffs of Northern France and Norway.

Overall conclusion: adequate coastal protection against sea level rise for the coming 300 years is completely feasible for NW Europe.



Figure 5.5 *Offshore sea dike in the case of excessive sea level rise of 2 to 10 m (sluice systems and offshore islands for ports/airports are included)*



Memo: Sea level rise
Date: September 2025





References

- Andreasen, J.R., Hogg, A.E., and Selley, H.L., 2023.** *Change in Antarctic ice shelf area from 2009 to 2019. The Cryosphere, Vol. 17, 2059-2072*
- De Conto, R.M. and Pollard, D., 2016.** *Contribution of Antarctica to past and future sea level rise. Doi: 10.1038/Nature 17145*
- Deltares 2007.** *Stijgend water : kan de Nederlandse delta standhouden? Report A0092.07 (in Dutch). Delft, Nederland*
- Deltares 2018.** *Mogelijke gevolgen van versnelde zeespiegelstijging voor het Deltaprogramma (in Dutch). Delft, Nederland*
- Deltares 2022.** *Sea Level monitor. Delft, The Netherlands*
- Medley, B. and Thomas, E.R., 2018.** *Increased snowfall over Antarctic Ice Sheet mitigated twentieth-century sea-level rise. Nature Climate Change. Letters; Doi.org/10.1038/s41558-018-0356-x*
- Morlichem, M., Goldberg, D., Bernes, J.M., Bassis, J.N., Benn, D.J., Crawford, A.J., Gudmundsson, G.H. and Seroussi, H., 2024.** *The West Antarctic Ice sheet may not be vulnerable to marine ice cliff instability during the 21st Century. Science Advances, Vol. 10, No. 34, August. Doi: 10.1126/sciadv.ado7794*
- Hoffman, J.S., P. U. Clark, A. C. Parnell, Feng He., 2017.** *Regional and global sea-surface temperatures during the last interglaciation. Science, 2017; 355 (6322): 276 DOI: 10.1126/science.aai8464.*
- TNO, 2007.** *Bodemdaling in Nederland. Rapport 2007-U-R0566B (in Dutch)*
- Vellinga, P., 1986.** *Dune erosion. Doctoral Thesis, Department of Civil Engineering, Delft University of Technology, Delft, The Netherlands*
- Yellow River Conservancy Press, 2004.** *Practice of Yellow River Control. China*

Websites

www.geo.uu.nl/fg
www.iceagenow.info
www.klimaatgek.nl
www.aviso.altimetry.fr
www.dmi.dk
www.knmi.nl
www.geocraft.com
www.nasa.gov
modis.gsfc.nasa.gov